

Journal of Visualized Experiments

A High-Throughput In Situ Method for Estimation of Hepatocyte Nuclear Ploidy in Mice --Manuscript Draft--

Article Type:	Invited Methods Article - JoVE Produced Video
Manuscript Number:	JoVE60095R2
Full Title:	A High-Throughput In Situ Method for Estimation of Hepatocyte Nuclear Ploidy in Mice
Section/Category:	JoVE Developmental Biology
Keywords:	Liver, polyploidy; hepatocyte; high-content imaging; hepatology; Hepatocyte nuclear factor 4 alpha (HNF4α); regeneration; injury repair
Corresponding Author:	Luke A. Noon CIBERDEM (Centro de Investigación Biomédica en Red de Diabetes y Enfermedades Metabólicas) Valencia, SPAIN
Corresponding Author's Institution:	CIBERDEM (Centro de Investigación Biomédica en Red de Diabetes y Enfermedades Metabólicas)
Corresponding Author E-Mail:	lnoon@cipf.es
Order of Authors:	Fátima Manzano-Núñez Ruby Peters Deborah J. Burks Luke A. Noon
Additional Information:	
Question	Response
Please indicate whether this article will be Standard Access or Open Access.	Standard Access (US\$2,400)
Please indicate the city, state/province, and country where this article will be filmed . Please do not use abbreviations.	Valencia, Spain

TITLE:**A High-Throughput In Situ Method for Estimation of Hepatocyte Nuclear Ploidy in Mice****AUTHORS AND AFFILIATIONS:**Fátima Manzano-Núñez¹, Ruby Peters², Deborah J. Burks^{1,3}, Luke A. Noon^{1,3}¹Centro de Investigación Príncipe Felipe (CIPF), Valencia, Spain²Department of Physiology, Development and Neuroscience, University of Cambridge, Cambridge, UK³Centro de Investigación Biomédica en Red de Diabetes y Enfermedades Metabólicas Asociadas (CIBERDEM), Madrid, Spain**Corresponding Author:**

Luke A. Noon (lnoon@cipf.es)

Email Addresses of Co-Authors:

Fátima Manzano-Núñez (fmanzano@cipf.es)

Ruby Peters (rp649@cam.ac.uk)

Deborah J. Burks (dburks@cipf.es)

KEYWORDS:

liver, polyploidy, hepatocyte, high-content imaging, hepatology, Hepatocyte nuclear factor 4 alpha (HNF4α)

SUMMARY:

We present a robust, cost-effective, and flexible method for measuring changes in hepatocyte number and nuclear ploidy within fixed/cryopreserved tissue samples that does not require flow cytometry. Our approach provides a powerful sample-wide signature of liver cytology ideal for tracking the progression of liver injury and disease.

ABSTRACT:

When the liver is injured, hepatocyte numbers decrease, while cell size, nuclear size and ploidy increase. The expansion of non-parenchymal cells such as cholangiocytes, myofibroblasts, progenitors and inflammatory cells also indicate chronic liver damage, tissue remodeling and disease progression. In this protocol, we describe a simple high-throughput approach for calculating changes in the cellular composition of the liver that are associated with injury, chronic disease and cancer. We show how information extracted from two-dimensional (2D) tissue sections can be used to quantify and calibrate hepatocyte nuclear ploidy within a sample and enable the user to locate specific ploidy subsets within the liver in situ. Our method requires access to fixed/frozen liver material, basic immunocytochemistry reagents and any standard high-content imaging platform. It serves as a powerful alternative to standard flow cytometry techniques, which require disruption of freshly collected tissue, loss of spatial information and potential disaggregation bias.

INTRODUCTION:

Hepatocytes in the mammalian liver can undergo stalled cytokinesis to produce binuclear cells, and DNA endoreplication to produce polyploid nuclei containing up to 16N DNA content. Overall cellular and nuclear ploidy increase during postnatal development, ageing and in response to diverse cellular stresses¹. The process of polyploidization is dynamic and reversible², although its precise biological function remains unclear³. Increased ploidy is associated with reduced proliferative capacity⁴, genetic diversity², adaptation to chronic injury⁵ and cancer protection⁶. Hepatocyte ploidy alterations occur as a result of altered circadian rhythm⁷, and weaning⁸. Most notably, the ploidy profile of the liver is altered by injury and disease⁹, and compelling evidence suggests that specific ploidy changes, such as increased $\geq 8N$ nuclei or loss of 2N hepatocytes, provide useful signatures for tracking non-alcoholic fatty liver disease (NAFLD) progression^{3,10}, or the differential impact of viral infections¹¹.

In general terms, liver injury and regeneration are associated with increased hepatocyte cell size and nuclear area¹², together with reduced overall numbers of hepatocytes, particularly those with 2N DNA content^{10,11}. Parenchymal injury in the liver is also frequently accompanied by expansion of non-parenchymal cells (NPCs), including stromal myofibroblasts, inflammatory cells and bipotent liver progenitor cells. High throughput methods that provide a quantitative cytological profile of parenchymal cell number and nuclear ploidy, whilst also accounting for changes in NPCs, therefore have considerable potential as research and clinical tools to track the response of the liver during injury and disease. Compelling recent in situ analysis of ploidy spectra in human samples of hepatocellular carcinoma also demonstrate that nuclear ploidy is dramatically increased within tumors and is specifically amplified in more aggressive tumor subtypes with reduced differentiation and loss of TP53¹³. Hence, there is a strong possibility that methodological advances in quantitative assessment of nuclear ploidy will assist in future prognostic profiling of liver cancer.

In this protocol, a flexible high-throughput methodology for the comparative analysis of mouse liver tissue sections is described, which provides detailed cytometric profiling of hepatocyte numbers, the NPC response and an internally calibrated method for estimating nuclear ploidy (**Figure 1**). Hepatocytes are distinguished from NPCs by hepatocyte nuclear factor 4 alpha (HNF4 α) immunolabelling, prior to characterization of nuclear size and nuclear morphometry. "Minimal DNA content" is estimated for all circular nuclear masks by integrating mean Hoechst 33342 intensity (a proxy for DNA density) with interpolated three-dimensional (3D) nuclear volume. Hepatocyte minimal DNA content is then calibrated using NPCs to generate a nuclear ploidy profile.

Image acquisition, nuclear segmentation and image analysis are performed using high-content imaging, enabling large areas of two-dimensional (2D) liver sections containing tens of thousands of cells to be screened. A custom-written program is provided for automated post-processing of high-content image analysis data to produce a sample-wide ploidy profile for all circular hepatocyte nuclei. This is performed using free to download software to calculate nuclear ploidy based on stereological image analysis (SIA)^{10,11,14,15}. The SIA methodology has been previously validated by flow cytometry as an accurate, albeit laborious, method for estimating hepatocyte

nuclear ploidy in the liver¹⁴, assuming circular nuclear morphology and a monotonic relationship between nuclear size and DNA content. In this protocol, both nuclear parameters are measured by assessment of nuclear morphometry and Hoechst 33342 labelling. Calculation of “minimal DNA content” for each nuclear mask is followed by calibration of hepatocyte nuclear ploidy using NPCs, which have a known 2–4n DNA content and therefore serve as a useful internal control.

Compared to conventional flow cytometry methods¹⁶ the approach described enables hepatocyte nuclear ploidy to be assessed in situ and does not require access to fresh tissue or disaggregation methods that can bias outcomes and be difficult to standardize. As with all SIA-based approaches, nuclear ploidy subclasses >2N are underrepresented by 2D sampling due to the sectioning of larger nuclei outside of the equatorial plane. The tissue-wide ploidy profile also describes minimum DNA content for all circular hepatocyte nuclear masks, and does not directly discriminate between mononuclear hepatocytes and binuclear cells that have two discrete (“non-touching”) nuclei of the same ploidy. However, the simplicity of this protocol allows considerable scope for it to be adapted to account for additional parameters such as internuclear spacing or cell perimeter analysis, that would facilitate identification of binuclear cells providing a more detailed assessment of cellular ploidy.

PROTOCOL:

All animal experiments were previously approved by the CIPF animal committee. Mice were housed in a pathogen-free facility at the Centro de Investigación Príncipe Felipe (Valencia, Spain), registered as an experimental animal breeder, user, and supply centre (reg. no. ES 46 250 0001 002) under current applicable European and Spanish animal welfare regulations (RD 53/2013).

1. Tissue harvesting and sample preparation

NOTE: This protocol describes how to freeze tissue without prior fixation or cryopreservation. For previously fixed/cryopreserved samples proceed to section 2 and omit step 3.1. All analyses have been performed using adult female C57BL/6 mice aged 12–16 weeks.

1.1. Sacrifice animals by fentanyl/pentobarbital intraperitoneal injection followed by cervical dislocation. With the mouse facing ventral side up, open the abdominal cavity and expose the liver by grasping the skin with tweezers and performing a vertical incision from the base of the lower abdomen to the base of the sternum using surgical scissors.

1.2. Carefully remove the gallbladder using fine tweezers, dissect out the liver and rinse the selected liver lobule in a 10 cm Petri dish plate filled with phosphate-buffered saline (PBS).

NOTE: It is recommended to compare the same liver lobe for each animal, in this case the median lobe was used.

1.3. Fill a labelled cryomold with optimal cutting temperature (OCT) medium at room temperature (RT). Avoid OCT bubbles. If they appear, push them to the edge of the mold using a

needle or pipette tip.

1.4. Embed liver lobule into a filled OCT cryomold and immediately place it on dry ice to ensure rapid freezing. Store cryomolds at -80 °C until cryosectioning.

2. Cryosectioning

2.1. Transport cryomolds on dry ice to avoid tissue degradation. Prior to cryosectioning equilibrate inside cryostat set to -20 °C for 20 min.

2.2. Eject sample by applying pressure to the base of the plastic cryomold. Apply liquid OCT to warm sample disk at RT, position in cryostat and attach an OCT embedded liver sample. Apply gentle pressure and wait 3 min for OCT to freeze ensuring the sample sticks to the disk.

NOTE: Avoid handling the sample with fingers as much as possible to evade tissue degradation.

2.3. Lock the sample into the arm of the cryostat and adjust the orientation so that the edge of the sample is parallel with the cryostat blade. Cut into the sample until tissue is reached.

2.4. Section the sample at 6 µm thickness. Place a labelled polyamide-coated slide over the sample for 5 s to let the sample stick onto the slide. Place the slide at RT for 3–5 min, then, for best results, proceed directly to section 3.

NOTE: For processing of multiple fresh-frozen samples reproducible results have been obtained by temporarily storing slides in a slide box on dry ice until all samples have been processed. When using this approach allow all slides to equilibrate to RT before proceeding to section 3. Formalin fixed paraffin embedded (FFPE) samples can be used, although background autofluorescence is increased by this method. To proceed from FFPE samples, section at 4 µm. Mount by catching sections from 40 °C water bath on polyamide-treated slides. Heat slides for 1 h at 60 °C, then deparaffinize by serial RT washes (5 min) in Coplin jars containing xylene (x2), ethanol 100% (x2), 96% (x2), 70% (x1) and dH₂O (x1). To expose antigens place slides in citrate buffer for 20 min at 90 °C before tempering slides in PBS at RT. Proceed to step 3.2.

3. Fluorescence immunolabelling

3.1. Fix tissue sections in a fume hood by applying 1 mL of 4% paraformaldehyde (PFA) in PBS for 10 min at RT. Transfer slides to a PBS filled Coplin jar and wash for 3 min using gentle agitation (repeat 3x).

NOTE: From now until the end of the immunostaining process, avoid drying of the sample.

3.2. Dry the area around each tissue section and surround using a hydrophobic pen. Permeabilize with 0.5% nonionic surfactant (i.e., Triton X-100) in PBS for 15 min at RT. Then wash in PBS filled Coplin jar for 3 min using gentle agitation (repeat 2x).

3.3. Block using a filtered solution of 1% bovine serum albumin (BSA), 5% horse serum, 0.2% nonionic surfactant in PBS (for at least 1 h at RT).

3.4. Incubate with primary HNF4 α antibody diluted in blocking buffer over night at 4 °C in a dark humid staining chamber (see **Table of Materials** for antibodies and specific dilutions).

3.5. Place slides into a PBS filled Coplin jar and wash for 3 min using gentle agitation (repeat 4x).

3.6. Incubate with Alexa-488 conjugated secondary antibody and Hoechst diluted in filtered 1% BSA and 0.2% nonionic surfactant in PBS for 2 h at RT in a dark humid staining chamber (see **Table of Materials** for antibodies and specific dilutions).

3.7. Place slides into a PBS filled Coplin jar and wash for 3 min using gentle agitation (repeat 4x). Wash in ddH₂O for 3 min using gentle agitation (repeat 2x).

3.8. Mount slides by placing two drops of fluorescent mounting media on a coverslip (24 x 60 mm) and laying slides over it, eliminating bubbles by applying gentle pressure. For long-term storage, seal coverslip at edges with clear nail polish and store in the dark at 4 °C.

3.9. Before proceeding, check slides using a conventional fluorescence microscope to ensure good fixation and immunolabeling.

NOTE: See **Figure 2A,B** for expected results.

4. Fluorescence image acquisition

NOTE: For this step, a high-content imaging platform (**Table of Materials**) is required that supports automatic fluorescence image acquisition.

4.1. Turn on the imaging system and open a new acquisition protocol.

4.2. Select the 10x objective, note the area of the field of view (in this case 0.6 mm²).

4.3. Set parameters to acquire fluorescence images using the appropriate excitation and emission filters (as per step 3.6). For Hoechst and Alexa-488, select "DAPI" and "GFP" channels with 390/18 and 438/24 nm excitation and 432.5/48 and 475/24 nm emission, respectively.

4.4. Focus the sample and ensure signal intensity is non-saturating. Ensure that image capturing is done with the same exposure time for all the images or use a system where the intensity of fluorescence is corrected for the exposure time.

4.5. Scan sample and acquire sufficient images to obtain complete coverage of the tissue section (approximately 20–50 fields of view, depending on the sample size).

4.6. Review the image database, manually eliminating (i) poorly focused fields, (ii) those at the borders of each tissue section (to avoid biasing cell density calculations), and (iii) those containing folded/physically damaged areas of the tissue section if present.

5. Automated fluorescence image analysis

NOTE: This step requires appropriate image analysis software (**Table of Materials**) capable of: (1) automatically identifying Hoechst labelled nuclei within images at 405 nm (nuclear segmentation), (2) assessing mean Hoechst nuclear intensity and morphometry, and (3) threshold analysis to determine the +/- status of nuclear fluorescence at 488 nm (HNF4 α). Some basic operator training/expertise is required to visually assess and adjust segmentation and thresholding parameters within the program to ensure that nuclei and HNF4 α +/- status are optimally gated (**Figure 2**).

5.1. In the image analysis software, open the acquisition file containing Hoechst (405 nm) and HNF4 α (488 nm) images from step 4.5, and create a new analysis protocol.

5.2. Define wavelengths to be used for nuclear segmentation (Hoechst, 405 nm) and for hepatocyte/NPC threshold analysis (HNF4 α , 488 nm).

5.3. Adjust the software's nuclear segmentation parameters (such as "minimum nuclear area" and nuclear detection "sensitivity") to ensure nuclei are optimally segregated.

NOTE: Good segmentation of hepatocytes should be prioritized over that of NPCs. Hepatocyte nuclei are characteristically rounded (interquartile size range: 40–64 μm^2). NPC nuclei, such as those of sinusoidal endothelia, are flattened/elliptical or irregular in shape and generally smaller and more closely packed than those of hepatocytes (interquartile size range: 30–43 μm^2). For mouse liver, minimal nuclear area $\geq 23 \mu\text{m}^2$ and detection "sensitivity" of 65% were used (see **Figure 2C,D** for expected results). Sensitivity determines how pixel clusters are recognized as individual nuclei based on their intensity and should be empirically tested for each sample set by the user before proceeding with automated image analysis.

5.4. Modify the threshold intensity at 488 nm to ensure optimal gating of hepatocytes (HNF4 α +) and non-parenchymal cells (HNF4 α -).

NOTE: See **Figure 2C,D** for expected results. The value of threshold intensity is relative and will depend on staining efficiency and acquisition settings such as laser intensity. It should therefore be standardized by the user. Use known HNF4 α - cells such as endothelial cells and periportal NPCs as an internal negative control and binuclear hepatocyte nuclei as a positive reference for staining. Test the analysis parameters using a small number of images to ensure good nuclear segmentation and intensity threshold segregation before applying analysis parameters to the entire dataset.

5.5. Select the following nuclear parameters to be quantified: (1) nuclear area based on Hoechst staining (μm^2), (2) mean nuclear Hoechst intensity (RU), (3) nuclear elongation factor (mean ratio of the short axis of the nucleus to the long axis of the nucleus, where a centre-symmetric [non-elongated] object has a value of 1, (4) Nuc 1/(form factor), mean nuclear “roundness” index calculated by perimeter $2/(4\pi \times \text{area})$. Values range from 1 to infinity, where 1 is a perfect circle, (5) HNF4 α status (positive-1 or negative-0), and (6) nuclear x/y coordinates based on “center of gravity” (cg), a method for locating the center of the object from greyscale images with sub-pixel precision.

5.6. Run the analysis for all sample datasets and export numerical data from step 5.5 to spreadsheet software.

6. Data analysis

NOTE: The data analysis step can be performed using any standard spreadsheet software.

6.1. Calculate hepatocyte and non-hepatocyte cell numbers.

6.1.1. Calculate the total area of liver section analyzed for each sample by multiplying the number of fields of view by the area of the field of view (step 4.2).

$$\text{Total area analyzed (A)} = \text{number of fields} \times \text{area of field of view}$$

6.1.2. Working with spreadsheet files generated for each liver section, filter the data by selecting only HNF4 α + nuclei. Calculate the total number of HNF4 α + nuclei analyzed and divide this by the total area analyzed to obtain mean hepatocyte density for each sample (**Figure 2F**).

$$\text{Mean hepatocyte density} = \frac{\text{total number of HNF4}\alpha \text{ positive nuclei}}{A}$$

6.1.3. Perform the same calculation for non-parenchymal cells by filtering the spreadsheet for HNF4 α - cells (**Figure 2E**).

6.2. Calculate hepatocyte nuclear size distribution.

6.2.1. Using spreadsheet software, filter data to select only HNF4 α + nuclei.

6.2.2. Plot values of nuclear area in a histogram (**Figure 2G**). Set the bin width to $5 \mu\text{m}^2$.

NOTE: Frequency values can be corrected for area (nuclei/ mm^2) as per step 6.1.1.

6.3. Perform hepatocyte nuclear ploidy analysis.

NOTE: The spreadsheet data from step 5.6 are used to generate a nuclear ploidy profile for each

sample. This process has been automated and can be performed using a custom written software that is freely available to download with supporting information and demonstration datasets at <https://github.com/lukeynoon> (see **Supplemental Files**). Source code is provided for users who wish to adapt the methodology. A description of the algorithm, together with instructions for installation and use are outlined below. The program uses spreadsheet data to automatically separate hepatocyte nuclei into two groups; (1) those with “simple” circular nuclei and (2) “complex” non-circular nuclei representative of binuclear cells with >2c ploidy. The minimal nuclear DNA content (a function of nuclear area and DNA density) is next calculated for all “simple” nuclei. A subsequent step then automatically calibrates HNF4α+ hepatocyte nuclear ploidy using HNF4α- nuclei as a known 2–4N internal control.

6.3.1. Download and install software.

6.3.1.1. Download the packaged application from: <https://github.com/lukeynoon>.

6.3.1.2. Launch MATLAB. Navigate to the APP tab of the toolstrip, click **Install App** and open the downloaded application termed “*Ploidy_Application.mlappinstall*”. A message will appear to confirm the successful installation.

NOTE: The application is now ready for use and will remain in the APP tab of the toolstrip.

6.3.2. Format input data.

NOTE: Prior to automated nuclear ploidy analysis, all spreadsheet files containing high content imaging data (step 5.6) should be stored and formatted according to the following instructions.

6.3.2.1. In each exported data file (.XLS 97-2004 workbook) from step 5.6, include a sheet termed “Cell measures” containing all the data required for the ploidy analysis set out in columns (**Figure 3A**). Ensure that the spreadsheet layout including column header names remains unchanged from that of **Figure 3A**, because the analysis method finds the correct column data by searching for these names (see demonstration datasets in **Supplemental Files** for reference). If for example, high-content image analysis software does not produce a “Light flux” column (**Figure 3A**), manually insert a “Light flux” column in the same location, i.e., column K and fill it with zeros.

6.3.2.2. For each experimental condition (e.g., “Injured-d14”), provide a control dataset, which will be used to calculate the internal control for 2–4N nuclear ploidy calibration (step 6.3.4.3). Here, select liver samples from untreated adult littermates (“Control-d0”; **Figure 3B–D**).

6.3.2.3. For biological replicates (per condition), store each spreadsheet in its own folder (as in **Figure 3B**). Name the folder prefixes incrementally, e.g., “Sample1, Sample2, Sample3... SampleN”, as per the filenames contained within. Hence, every dataset folder (e.g., “Control-d0”) should contain a series of subfolders (“Sample1”, “Sample2”, etc.) each containing a spreadsheet file of the same corresponding name.

6.3.3. Run the application.

6.3.3.1. Within MATLAB, launch the “Ploidy_Application” by clicking on the icon within the MY APPS tab of the toolbar (**Figure 3C**). The Ploidy_Application graphical user interface (GUI) will appear (**Figure 3C**).

6.3.3.2. Click the **Path to control data** button to navigate to the folder in which the control data replicates reside (e.g., “Control-d0”). This data path will then appear in the interface (e.g., */Users/Desktop/Control-d0*).

6.3.3.3. Next, in “folder prefix” type the name to be given to the output files (e.g., “Sample”).

NOTE: This prefix can be changed to any text, provided that the folders and filenames remain incrementally named.

6.3.3.4. Click the **Path to other data** button and navigate to the folder in which the comparative data replicates reside (e.g., “Injured-d14”). This data path will then appear in the interface (e.g., */Users/Desktop/Injured-d14*).

6.3.3.5. Click **Run!**. When the analysis is complete, the status bar will read “Analysis Complete!..”.

NOTE: The application will report, for each sample, stratification of “simple” nuclei into $\leq 2n$, $2n-4n$, $4n-8n$ and $8n+$ in terms of absolute counts and as a percentage of total (**Figure 3D**). These files will be automatically saved in each sample folder as: “Count_2n.txt”, “Count_2n_to_4n.txt”, “Count_4n_to_8n.txt”, “Count_8n_and_higher.txt”, “Percentage_2n.txt”, “Percentage_2nto4n.txt”, “Percentage_4nto8n.txt”, “Percentage_8n_and_higher.txt”. The Ploidy_Application will automatically save a list for each sample, of all the individual ploidy estimates for “simple” hepatocyte and non-hepatocyte nuclei in “Ploidy_All_Hepatocytes.txt” and “Ploidy_NonHepatocytes.txt”. For the control dataset, the method also saves the minimal DNA content thresholds calculated for stratification of ploidy (see step 6.3.4.3.7) in a file named “Normalised_Thresholds_Control”. Finally, the application will produce a folder for both the control and the selected comparative condition data termed “Summary”. This folder contains two subfolders, “Ploidy” and “Stratification” which contain the averages of all samples provided (**Figure 3D**).

6.3.4. Description of the methodology

NOTE: The following section describes in detail the methodology used by the Nuclear Ploidy Analysis software. If the user chooses not to use the application, these steps can be followed using spreadsheet software to calculate the nuclear ploidy profile manually.

6.3.4.1. Separate nuclei into “simple” or “complex” according to nuclear morphometry.

6.3.4.1.1. Calculate a “circularity index” for all nuclei, defined as the nuclear “elongation factor”

divided by the “Nuc 1/(form factor)”, where a value of 1.0 indicates a perfect circle.

NOTE: “Nuclear elongation” and “Nuc 1/(form factor)” are two discrete measures of an object’s “circularity” that assess complementary, non-overlapping morphometric criteria. The former measures the long- and short-axes of an object, while the latter compares the length of perimeter of an object to that of its area. To strengthen the definition of nuclear circularity used in this protocol, these two measurements have been combined into a single “circularity index”. A previous approach to estimate nuclear ploidy using the described methodology used only nuclear elongation¹⁷. While acceptable results were obtained using this approach, the authors have observed that a composite “circularity index” improves discrimination of manually selected nuclei from mononuclear and binuclear hepatocytes (data not shown).

6.3.4.1.2. Classify nuclei with a circularity index ≤ 0.8 as “complex” and those > 0.8 as “simple”.

6.3.4.2. Estimate “minimal” DNA content (m) for all “simple” nuclei.

6.3.4.2.1. Calculate the nuclear radius (r) using the formula:

$$\text{Nuclear radius } (r) = \sqrt{\frac{\text{nuclear area}}{\pi}}$$

6.3.4.2.2. Calculate nuclear volume (v) using the volume of a sphere formula:

$$\text{Nuclear volume } (v) = \frac{4}{3} \times \pi \times r^3$$

6.3.4.2.3. Generate a relative value for minimal DNA content (m) using the formula:

$$\text{Minimal DNA content } (m) = \text{Mean Hoechst intensity} \times v$$

6.3.4.3. Calibrate the dataset using the NPC (HNF4 α -) nuclei as an internal 2–4N control.

NOTE: NPCs have a 2–4N DNA content depending on cell cycle status. Hence, the mean value of NPC “minimal” DNA content (NPC_m) increases with injury (**Figure 4A**). Calibration error is minimized by establishing an upper limit of NPC_m representing a 4c threshold (**Figure 4B**).

6.3.4.3.1. Within the spreadsheet, select only NPC nuclei with values for “m” that lie within 1 standard deviation (SD) of the mode (this filters out noise from possible segmentation error).

6.3.4.3.2. Within this filtered range, examine nuclear areas and their corresponding mean Hoechst intensities (**Figure 4C**).

6.3.4.3.3. Estimate the smallest nuclear area within this filtered range with maximal nuclear

Hoechst intensity (i.e., the point at which the line of the curve changes direction in the filtered dataset as illustrated by the red circle in **Figure 4C**). This value represents a 2N–4N transitional state (t) above which sampling of 4c nuclei predominates over 2c nuclei, resulting in a maxima of mean Hoechst intensity.

NOTE: This value is automatically determined by the software; however, spreadsheet users can manually select this point as the transitional size.

6.3.4.3.4. Calculate the minimal DNA content represented by this transitional size (t_m) by following step 6.3.4.2.

6.3.4.3.5. To estimate the 4N shoulder of the NPC_m dataset, add 1 SD to the value of t_m . The resulting number (**Figure 4B**) describes the upper limit of NPC minimal DNA content to be used for nuclear ploidy stratification (S_{4c}).

6.3.4.3.6. Repeat steps 6.3.4.3.1–6.3.4.3.5 for all “control” samples.

NOTE: For example, in **Figure 3**, uninjured control livers (“Control-d0”) are used as a control condition.

6.3.4.3.7. Calculate an average 4c stratification threshold (S_{4c}) for “control” samples and use this to extrapolate the 2c (S_{2c}) and 8c (S_{8c}) boundaries for minimal DNA content (m). Stratification thresholds are automatically generated and stored by the software (step 6.3.3.3).

NOTE: Depending on the study design, the average stratification threshold values may be calculated for each condition or for specific conditions (e.g., healthy control liver). However, the Nuclear Ploidy Analysis software requires that one of a set of 2 files is designated as “control” for the purposes of calculating relative ploidy values.

6.3.4.3.8. Calculate a ploidy value for all nuclei using the S_{2c} value generated in step 6.3.4.3.7 as per:

$$Ploidy (p) = \frac{Minimal\ DNA\ content\ (m)}{S_{2c}} \times 2$$

6.3.4.3.9. Stratify “simple” hepatocyte (HNF4α+) nuclei into 2c/4c/8c/>8c brackets according to the following criteria: “2c” HNF4α+ = $p \leq 2$; “4c” HNF4α+ = $2 < p \leq 4$; “8c” HNF4α+ = $4 < p \leq 8$; “>8c” HNF4α+ = $8 < p$.

6.3.4.3.10. To reconstruct the spatial patterning of ploidy subgroups, separate the nuclear data within each sample spreadsheet according to the corresponding fields in which they were acquired. Then use associated nuclear x/y coordinates (from step 5.5) to plot ploidy subgroups in 2D (**Figure 5C**).

REPRESENTATIVE RESULTS:

This method has been used to measure the impact of cholestatic injury on the adult mouse liver by feeding animals for 0–21 days with a hepatotoxic diet containing 0.1% 3,5-diethoxycarbonyl-1,4-dihydrocollidine (DDC)¹⁷. Chronic DDC feeding results in hepatocellular injury increased ploidy and periportal expansion of NPCs. The user should be aware that mouse strain and age-dependent differences may exist in nuclear ploidy and that all analyses have been performed using adult female C57BL/6 mice aged 12–16 weeks.

After HNF4 α immunolabelling (protocol section 3), it is important to check all slides using conventional fluorescence microscopy, to ensure good quality fixation and staining (**Figure 2A**). Smearing or blurring of Hoechst can indicate inadequate fixation or sample degradation prior to fixation (**Figure 2B**), in which case return to protocol section 2 and shorten the time between sectioning and fixation (step 3.1). Successful immunolabelling with the HNF4 α antibody can easily be judged at this stage by clear discrimination of positively labelled hepatocyte nuclei, typically larger and more rounded than those of NPCs (**Figure 2A**). Flattened/elliptical endothelial nuclei within the parenchyma, or dense patches of cells that expand in periportal areas following DDC injury can serve as a useful visual reference for identifying HNF4 α - NPCs when assessing the success/failure of immunostaining.

Nuclear segregation and HNF4 α threshold parameters (steps 5.2–5.4) should be carefully optimized prior to automatic image analysis (step 5.6) to broadly reflect the visual pattern of immunostaining observed by conventional fluorescence microscopy at the end of protocol section 3 (**Figure 2C**). Examples of optimal vs suboptimal nuclear segmentation and HNF4 α threshold protocols are summarized in **Figure 2D**. Following image analysis (step 6.1.3), the data should reflect increasing numbers of NPCs in the liver with DDC injury (**Figure 2E**), from 52% \pm 2.0% of nuclei in control livers to 72.8% \pm 1.4% after 21 days of DDC treatment. Hepatocytes represent 48.0% \pm 2.0% of total nuclei in control livers, concordant with previous analyses of liver histology showing that hepatocytes occupy 70–85% of the tissue volume, but only 45–50% of total liver cells^{18,19}. A small but significant reduction in numbers of HNF4 α + nuclei is observed during the first 14 days of DDC feeding (**Figure 2F**). A frequency distribution plot of hepatocyte nuclear area (step 6.2) shows a peak HNF4 α + nuclear area in control livers in the 40–50 μm^2 size range, and a clear right-shift in nuclear size after DDC injury (**Figure 2G**); consistent with increased ploidy and hepatocellular hypertrophy¹².

In healthy (day 0) control livers, 63.4% \pm 1.7% of HNF4 α + nuclei have a “simple” circular morphometry (**Figure 5A**). This figure decreases to 46.8% \pm 5.7% ($P = 0.042$) after 21 days of DDC injury, reflecting increased complexity in nuclear morphometry presumably associated with shifting between ploidy states during polyploidization (see “Interpretation of nuclear morphometry” below). Representative examples of nuclear ploidy distributions obtained using this method in control liver sections are shown in **Figure 5A**, which describes how interpolation of DNA content allows stratification of individual cells within a single sample. Mean values for subsets of “complex” and “simple” HNF4 α + cells are also shown (**Figure 5A**). The data are consistent with previous estimates of polyploidy in 80–90% of adult murine hepatocytes². The frequency of complex nuclei (36.6% \pm 1.7%) in control livers also approximates to that of

binuclear cells (35%)²⁰, though data should be strictly regarded as a measure of nuclear rather than cellular ploidy (see “Interpretation of nuclear morphometry” below). Comparison of relative ploidy between control (day 0) and DDC treated groups should reflect significant loss of 2c and 4c hepatocyte nuclei with injury together with increased numbers of >8c cells (**Figure 5B**). Relative positional information for each ploidy subgroup can be interrogated by scatter plot of x-y coordinates associated with each nucleus within the dataset or by retrieving the 2D location of particular hepatocyte subsets within the high-content image analysis software (**Figure 5C**).

Calibration

To assess the validity of the NPC calibration method used, dual immunolabeling of liver sections was performed using antibodies to HNF4 α and proliferative marker Ki-67 (**Figure 6A,B**). These data showed enrichment for Ki-67, which labels cells in all active phases of the cell cycle, on the right side of the NPC minimal DNA distribution curve (between S_{2c} and S_{4c}) – where NPCs would be expected to be replicating DNA and therefore have >2c ploidy (**Figure 6A**). After internal calibration of all control and injured liver samples studied, Ki-67, was significantly enriched ($P < 0.0001$) in “simple” NPC nuclei with an estimated ploidy of >2c ($82.5\% \pm 6.6\%$ SD, $n = 12$) compared to those with $\leq 2c$ ploidy ($17.5\% \pm 6.6\%$ SD, $n = 12$) (**Figure 6B**), indicating successful ploidy calibration. These data support the validity of the method used. Also, assuming accurate thresholding of Ki67, they provide some quantitative insight into the extent to which subequatorial nuclear masks from higher ploidy groups “contaminate” groups below.

To further test the validity of the NPC calibration method, an external calibrator was introduced based on the previously reported nuclear volume of mouse 2N hepatocytes ($155.8 \mu m^3$)¹⁴. When this figure was used in combination with an average value of Hoechst intensity for HNF4a- nuclei the resulting estimate for mean hepatocyte ploidy in the control livers was indistinguishable from that of the internal (S_{2c}) calibrator (**Figure 6C**). Moreover, estimates of mean hepatocyte ploidy in mice of the C57BL/6 mouse strain of comparable age, were also similar, confirming that prior empirical knowledge of 2N hepatocyte nuclear size is not required, making this internally controlled methodology for estimating nuclear ploidy fully autonomous.

Interpretation of nuclear morphometry

The method described provides a ploidy readout for hepatocyte nuclei with “simple” circular morphometry. Exclusion of “complex” nuclei is based on the hypothesis that they represent a proportion of binuclear hepatocytes with overlapping/touching nuclear masks, making accurate ploidy determination for this subset more challenging (**Figure 7A**). Importantly, segregation of nuclei according to circularity does not enable the user to distinguish between the nuclei of mononuclear hepatocytes and those of binuclear cells, in which two nuclei of similar ploidy are clearly separated within the cell. This was empirically tested by manually selecting binuclear and mononuclear cells from the image datasets and assessing their segregation by the algorithm (**Figure 7B**). Nuclei of binuclear hepatocytes that were physically close (**Figure 7C**) but “not touching” were categorized by the algorithm as “simple”, whereas those that were “touching” were clearly discriminated as “complex”. Hence, this assay does not provide a readout of cellular ploidy in the liver, given that nuclei of binuclear cells are subdivided between the “simple” and “complex” subclasses (see discussion). However, some insight into the switching between states

of cellular and nuclear ploidy may be gained from this data simply by plotting histograms of nuclear morphometry and nuclear size and applying a model of how “complex” and “simple” states are transitioned between during polyploidization (**Figure 7D**). In control livers three phases (I–III) of nuclear morphometry are clearly observed (**Figure 7E**). They represent the clustering of circular 2N (I), 4N (II) and 8N (III) nuclear masks respectively (as illustrated in **Figure 7D**). Mononuclear 16N hepatocytes are extremely rare in adult mouse livers^{16,18,21}, hence the 16N cellular ploidy group is comprised almost entirely of binuclear cells with 8N nuclei, located within, and to the right, of phase III (**Figure 7E**), explaining the drop in circularity to the right of phase III. Interestingly, upon injury (DDC day 14), a quantitative shift towards increased complexity (“binuclearity”) begins in phases I (reflecting 2n to 2x2n) and phases III (reflecting 8n to 2x8n), before it is finally consolidated in all three phases (I–III). The authors speculate that this shift towards increased complexity is due to an increased cellular ploidy resulting from stalled cytokinesis, whereas to the right of phase III the opposite trend is observed, due to increased representation of circular 16N mononuclear cells in the injured liver due to endoreplication. These observations will of course need to be tested by adapting the method to properly account for cellular ploidy (see discussion).

FIGURE LEGENDS:

Figure 1: Summary of workflow. Liver tissue is harvested (1), cryosectioned (2), fixed and immunolabelled with an HNF4α antibody allowing for parenchymal and non-parenchymal cells (NPCs) to be discriminated (3). Once processed, samples are digitized using a high-content imaging platform using automated image capture (4) and analysis (5). Cells are segmented by Hoechst nuclear fluorescence and HNF4α immunofluorescence thresholding. Next, Hoechst nuclear area (“A”) and circularity (“C”) are calculated. Finally, the data are analyzed (6); HNF4α-NPCs are quantified (i) and HNF4α+ hepatocyte nuclei are separated into two subsets (“simple” and “complex”) according to nuclear circularity (ii). Interpolation of hepatocyte nuclear ploidy is then performed for all “simple” nuclei as a function of nuclear radius (r) and mean Hoechst fluorescence intensity (as a proxy for nuclear DNA density) (iii). The data are then stratified using NPCs as an internal 2N calibrator (iv) before compiling a sample summary (v).

Figure 2: High-content image analysis and cytometric profiling of the mouse liver during chronic DDC feeding. (A) A representative confocal image of HNF4α/Hoechst immunofluorescence staining of the adult mouse liver after 21 days of feeding with a diet containing 0.1% DDC; image shows rounded HNF4α+ hepatocyte nuclei (“H”) and expansion of HNF4α- NPCs in areas surrounding the portal vein (“PV”). (B) Examples of optimal (“correct”) and suboptimal (“incorrect”) nuclear Hoechst staining indicating poor fixation. (C) Use of high-throughput image analysis platform to segregate hepatocytes and NPCs according to nuclear Hoechst staining and HNF4α immunolabelling. Software masks (red/green lines) show how nuclei are correctly segmented according to Hoechst fluorescence and sorted into hepatocytes (+) or NPCs (-) according to HNF4α status. (D) A guide to optimizing the setup for segmentation/threshold analysis. Superimposed nuclear masks recognized by the software are indicated by green/blue lines for nuclear segmentation and green/blue (HNF4α+) or red/blue (HNF4α-) for threshold analysis (H = hepatocyte). Troubleshooting: Nuclear detection sensitivity set too low (i), or too

high (ii). Threshold for HNF4 α set too low (iii), or too high (iv). **(E,F)** Quantitative analysis of NPC and hepatocyte nuclei during DDC feeding: **(E)** HNF4 α - and **(F)** HNF4 α + nuclear densities are compared against time of DDC treatment (days). A total of 5.7×10^5 cells were analyzed, from 4–6 animals per timepoint. Data are presented as mean + SEM. **P < 0.01 and ***P < 0.001. One-way ANOVA was used to compare means. Significance P values were calculated using Fisher's least significant difference (LSD) test. **(G)** Frequency distribution of HNF4 α + nuclear area during DDC treatment. The data show a right-shift in hepatocyte nuclear area during injury consistent with cellular hypertrophy and polyploidization. A total of 2.5×10^5 HNF4 α + nuclei were analyzed, from 4–6 animals per timepoint. This figure has been modified from Manzano-Núñez et al.¹⁷.

Figure 3: Automated analysis of hepatocyte nuclear ploidy using custom written software. **(A)** Screenshot showing correct formatting of spreadsheet data for input into the nuclear ploidy analysis software. Columns containing essential data (step 5.5 of the protocol) are highlighted yellow. All column titles should precisely match those indicated. **(B)** Screenshot showing how individual spreadsheet files containing data from biological replicates ("Sample1", "Sample2", etc.) should be named and organized in subfolders for each condition (entitled "Control-d0" and "Injured-d14" in this example). **(C)** Screenshot after successful installation of the ploidy application (red circle). When the application is launched (by clicking "Ploidy_Appl..") in the MY APPS tab of the toolbar the "Ploidy_GUI" appears (lower panel). The experiment name ("Sample") and paths to the control (e.g., "Control-d0") and test (e.g., "Injured-d14") datasets are entered before clicking **Run**. The software then calculates, calibrates and stratifies nuclear ploidy for all samples using the "Control-d0" dataset to generate thresholds for minimal DNA content. **(D)** Data output from Ploidy_Application shows individual data files automatically saved in each sample folder (i) containing absolute and percentage numbers of "simple" nuclei in each ploidy group. For each condition (in this case both "Control-d0" and "Injured-d14"), a summary folder is also automatically generated containing mean nuclear ploidy estimates for all "simple" hepatocyte and non-hepatocyte nuclei (ii) and a breakdown of how nuclear ploidy is stratified for each sample (iii).

Figure 4: The use of NPCs as an internal ploidy calibrator. **(A)** Graph showing the impact of DDC injury on mean minimal DNA content (m) of hepatocyte (HNF4 α +) and NPC (HNF4 α -) nuclei. All data are normalized to day 0 NPCs ($n = 4$ animals per timepoint). **(B)** Histogram describing the distribution of NPC $_m$ values in a single representative liver sample (day 0, total of 7,180 nuclei). The schematic (above) shows how circular NPC masks can derive from cells with a 2–4c DNA content. The aim of the calibration method is to define the stratification threshold representing 4c (S_{4c}) at the upper limit of the NPC $_m$ distribution (dotted line), while minimizing noise due to segmentation errors at the extremes of the distribution curve. **(C)** Changes in mean Hoechst intensity and nuclear area for NPC (HNF4 α -) nuclei are plotted. To avoid segmentation error only those nuclei with a corresponding NPC $_m$ value of within 1 SD of the mode NPC $_m$ value are scrutinized (yellow box). Within this range the 2c–4c transition size (t) is calculated and used as an anchor point within the data to estimate the S_{4c} .

Figure 5: High-throughput in situ analysis of nuclear ploidy in the mouse liver during chronic

DDC feeding. (A) Analysis of control adult liver using the described methodology. HNF4 α + hepatocyte nuclei from 2D liver sections are subdivided according to Hoechst nuclear circularity into two groups: “simple” and “complex”. (Top) Representative fluorescence Hoechst images of cells belonging to these two groups are shown. (Left) Scatterplot showing stratification of simple HNF4 α + nuclei from one sample (day 0) according to interpolated ploidy value, nuclear area and mean nuclear Hoechst intensity. (Right) Pie chart detailing the typical breakdown of HNF4 α + cells in control liver (day 0) indicating the proportions of each nuclear ploidy subclass. A total of 6.7×10^4 HNF4 α + nuclei from 4 animals were analyzed. (B) Impact of DDC liver injury on hepatocyte nuclear ploidy by high-throughput in situ analysis. Graphs demonstrate the relative decrease in the proportion of 2c and 4c hepatocyte nuclei within the first 14 days of DDC feeding while >8c polyploid nuclei dramatically increase in number. A total of 1.5×10^5 HNF4 α + nuclei were analyzed (n = 4 animals per timepoint). Data are presented as mean + SEM. **P < 0.01 and ***P < 0.001. One-way ANOVA was used to compare means. Significance P values were calculated using Tukey’s multiple comparison test. (C) Example to show how nuclear ploidy subclasses can be spatially tracked within the parenchyma using this method, by interrogating high-content imaging data with the same quantitative criteria used for ploidy stratification (circularity, nuclear size and mean Hoechst intensity). Hoechst fluorescence images are shown with software masks (red dots) marking 2c nuclei in the liver at two timepoints during chronic DDC feeding (day 14 and 21). Portal vein (blue dotted line) and periportal areas in which NPCs expand (yellow line) are indicated.

Figure 6: Critical assessment of the NPC calibration method. (A,B) Proliferating NPCs are successfully categorized with a >2c ploidy score. (A) Histogram of NPC minimal DNA content from control livers immunolabeled with antibodies to HNF4 α and proliferative marker Ki-67 (n = 4, data are presented as mean + SEM). Stratification thresholds for 2c (S_{2c}) and 4c (S_{4c}) are indicated. (B) Stratification of NPCs according to the described methodology results in a significant enrichment of Ki-67 immunolabelling in nuclei assigned a >2c ploidy score (n = 12). Data are presented as mean + SEM. Unpaired t test was used to compare the means ****P < 0.0001. (C) External validation of the NPC calibration method. Estimates of mean hepatocyte nuclear ploidy obtained using the internal NPC calibrator method were compared to those obtained by calibration of the same samples (Control C57BL/6 mouse liver 3–4 months, n = 4) with a known nuclear volume for 2N hepatocytes¹⁴. Data is also presented from two independent analyses^{21,22} describing hepatocyte nuclear ploidy from mice of the same strain at ages 2–6 months (shown to the right of the dotted line).

Figure 7: Hepatocyte nuclear morphometry has a “complex” relationship with cellular ploidy. (A) Summary of how hepatocyte cellular ploidy (2N, 4N, 8N and 16N) is partially segregated by 2D analysis of nuclear morphometry. Binuclear cells (red) are subdivided between “simple” (“S”) and “complex” (“C”) morphometries depending on whether nuclei appear to be touching or not. (B,C) Individual hepatocytes were manually selected and analyzed for nuclear morphometry and internuclear spacing. (B) Binuclear hepatocytes with “touching” nuclei were “complex” (100% ≤ 0.8), whereas mononuclear cells (black) and binuclear hepatocytes with non-touching nuclear masks were “simple” (94% > 0.8). (C) “Simple” nuclei of binuclear hepatocytes could be distinguished from those of mononuclear cells on account of significantly reduced inter-nuclear

spacing ($n = 3$, total of 94 nuclei analyzed). (D) Model approximating how cellular ploidy states from panel A might be distributed in terms of 2D nuclear morphometry and nuclear area resulting in clustering of simple circular forms into four phases (I–IV). (E) Comparison of HNF4 α + nuclear morphometry/size plots in control livers (day 0) and after 14 days (left) and 21 days (right) of DDC injury. Morphometry phases are indicated above (I–V). Arrows indicate shifts in nuclear morphometry resulting from injury that are consistent with binuclearization of 2c (“a”), 4c (“b”) and 8c (“c”) nuclei, together with increased mononuclearization of the 16N cellular ploidy class (d). Total of 29–30 $\times 10^3$ nuclei analyzed per condition ($n = 2$).

DISCUSSION:

A high-content, high-throughput approach for the analysis of tissue remodeling and estimation of hepatocyte nuclear ploidy in the murine liver is described. Once familiar with the procedure, a user can process, image and analyze multiple samples in a 3–5 day period, generating large testable datasets that provide a detailed signature of liver health. Given the simplicity of the sample preparation method, together with the large numbers of cells and tissue area analyzed (on average 14 mm²/sample), results are robust and highly reproducible. Automation of image capture and analysis also removes user error and potential bias from these important steps. An important innovation is the use of NPCs as an internal ploidy calibrator that enables relative assessment of hepatocyte nuclear DNA content both within and between samples. Incorporation of an HNF4 α labelling step is therefore key to providing this protocol with a unique technical advantage compared to previously published 2D methods^{3,12,22}. In contrast, the relative simplicity of the methodology in comparison with 3D reconstruction workflows¹⁸ makes it technically less laborious and potentially more flexible.

Compared to the precision method of flow cytometry, an important caveat to extrapolating nuclear DNA content from 2D tissue sections, is the limited confidence that can be attributed to the categorization of individual nuclei with regards to ploidy status. Added to this is the inherent bias within SIA based approaches to overrepresent smaller ploidy subgroups due to subequatorial sampling. However, by normalizing data to an internal standard and taking a large population based approach, the error due to these effects is mitigated and comparable across samples. Hepatocytes are characterized by a highly rounded nuclear morphology, compared to for example NPCs, meaning they are particularly amenable to accurate estimation of DNA content based on nuclear cross-sectional area alone^{10,11,14,15,23}. The SIA-based approach has been refined in this protocol to account both for nuclear circularity and DNA density by integrating measures of morphometry and mean Hoechst fluorescence intensity resulting in an estimated “minimal DNA content” descriptor for individual nuclei. Importantly, the use of NPCs as a 2–4N ploidy control provides an important internal standard for objective calibration and stratification of minimal nuclear DNA content, making the methodology described applicable to samples of any species, or format, given that an appropriate antibody for HNF4 α (or similar hepatocyte nuclear marker) can be sourced.

Although assessment of nuclear ploidy has been shown to provide useful signatures for liver disease progression^{10,13}, in order to fully ascertain the diversity of ploidy changes within the liver it would be both desirable and necessary to adapt the described methodology to account for

hepatocellular perimeter and thus cellular ploidy. Mapping of cellular ploidy has previously been achieved by labelling of the hepatocyte perimeter using markers such as beta catenin^{10,13,24}, actin^{12,22} and cytokeratin^{10,11} in human and mouse liver samples. However, when this was tested after DDC injury, dramatic epithelial remodeling precluded reliable assessment of hepatocellular perimeter both by phalloidin (data not shown) or antibodies to beta catenin¹⁷. Hence, whilst this approach is feasible, it may not be applicable to all injury models, but if achieved would advance mapping of cellular ploidy as well as making estimates of hepatocyte size and number more accurate. It also remains plausible that by accounting for additional nuclear parameters, such as internuclear spacing (**Figure 7C**), mononuclear cells could be discriminated from “simple” binuclear hepatocytes, and that further segregation of “complex” binuclear cells could be achieved by radial measurements of the nuclei that their 2D masks contain.

Given that validated human HNF4 α antibodies exist for FFPE tissue²⁵ and that internal calibration frees this methodology of any species-specific limitations, the protocol is almost immediately applicable to human samples. Thus, it has considerable potential to provide a benchmark for high-throughput analysis of hepatocyte nuclear ploidy and liver injury in human disease. Also, by multiplexing with other antibodies, this method can reveal new roles for particular hepatocyte subsets and their response to liver injury and disease. To this end, we have successfully combined the methodology with immunostaining for the proliferative nuclear marker Ki-67 (**Figure 6**), which enables useful information to be gleaned – including identification of non-proliferating 2N populations of NPCs for improved internal calibration of ploidy (Noon, unpublished data 2019). Hence, by coupling flexibility with the positional and quantitative data that the method provides, we suggest that its future applications will improve understanding of the role of polyploidy in the liver.

ACKNOWLEDGMENTS:

This work was funded by the Spanish MINECO Government grants BFU2014-58686-P (LAN) and SAF-2017-84708-R (DJB). LAN was supported by a national MINECO Ramón y Cajal Fellowship RYC-2012-11700 and FMN by a regional Vall+D studentship of the Valencian Generalitat ACIF/2016/020. RP would like to acknowledge Prof. Ewa K. Paluch for funding. We thank Dr. Alicia Martínez-Romero (CIPF Cytometry service) for help with the IN cell platform.

DISCLOSURES:

The authors have nothing to disclose.

REFERENCES:

1. Gentric, G., Desdouets, C. Polyploidization in liver tissue. *American Journal of Pathology*. **184** (2), 322–331 (2014).
2. Duncan, A.W. et al. The ploidy conveyor of mature hepatocytes as a source of genetic variation. *Nature*. **467** (7316), 707–710 (2010).
3. Gentric, G., Desdouets, C. Liver polyploidy: Dr Jekyll or Mr Hide? *Oncotarget*. **6** (11), 8430–1 (2015).
4. Wilkinson, P.D. et al. The Polyploid State Restricts Hepatocyte Proliferation and Liver Regeneration in Mice. *Hepatology*. **69** (3), 1242–1258 (2019).

788 5. Wilkinson, P.D. et al. Polyploid Hepatocytes Facilitate Adaptation and Regeneration to Chronic
789 Liver Injury. *The American Journal of Pathology*. **189** (6), 1241–1255 (2019).

790 6. Zhang, S. et al. The Polyploid State Plays a Tumor-Suppressive Role in the Liver. *Developmental*
791 *Cell*. **44** (4), 447–459.e5 (2018).

792 7. Chao, H.-W. et al. Circadian clock regulates hepatic polyploidy by modulating Mkp1-Erk1/2
793 signaling pathway. *Nature Communications*. **8** (1), 2238 (2017).

794 8. Celton-Morizur, S., Merlen, G., Couton, D., Margall-Ducos, G., Desdouets, C. The insulin/Akt
795 pathway controls a specific cell division program that leads to generation of binucleated
796 tetraploid liver cells in rodents. *Journal of Clinical Investigation*. **119** (7), 1880–1887 (2009).

797 9. Wang, M.J., Chen, F., Lau, J.T.Y., Hu, Y.P. Hepatocyte polyploidization and its association with
798 pathophysiological processes. *Cell Death & Disease*. **8** (5), e2805 (2017).

799 10. Gentric, G. et al. Oxidative stress promotes pathologic polyploidization in nonalcoholic fatty
800 liver disease. *Journal of Clinical Investigation*. **125** (3), 981–992 (2015).

801 11. Toyoda, H. Changes to hepatocyte ploidy and binuclearity profiles during human chronic viral
802 hepatitis. *Gut*. **54** (2), 297–302 (2005).

803 12. Miyaoka, Y. et al. Hypertrophy and Unconventional Cell Division of Hepatocytes Underlie Liver
804 Regeneration. *Current Biology*. **22** (13), 1166–1175 (2012).

805 13. Bou-Nader, M. et al. Polyploidy spectrum: a new marker in HCC classification. *Gut*. gutjnl-
806 2018-318021 (2019).

807 14. Danielsen, H., Lindmo, T., Reith, A. A method for determining ploidy distributions in liver
808 tissue by stereological analysis of nuclear size calibrated by flow cytometric DNA
809 analysis. *Cytometry*. **7** (5), 475–480 (1986).

810 15. Guidotti, J.-E. et al. Liver Cell Polyploidization: A Pivotal Role for Binuclear
811 Hepatocytes. *Journal of Biological Chemistry*. **278** (21), 19095–19101 (2003).

812 16. Severin, E., Meier, E.M., Willers, R. Flow cytometric analysis of mouse hepatocyte ploidy - I.
813 Preparative and mathematical protocol. *Cell and Tissue Research*. **238** (3), 643–647 (1984).

814 17. Manzano-Núñez, F. et al. Insulin resistance disrupts epithelial repair and niche-progenitor Fgf
815 signaling during chronic liver injury. *PLoS Biology*. **17** (1), e2006972 (2019).

816 18. Morales-Navarrete, H. et al. A versatile pipeline for the multi-scale digital reconstruction and
817 quantitative analysis of 3D tissue architecture. *eLife*. **4**, e11214 (2015).

818 19. Baratta, J.L. et al. Cellular organization of normal mouse liver: A histological, quantitative
819 immunocytochemical, and fine structural analysis. *Histochemistry and Cell Biology*. **131** (6), 713–
820 726 (2009).

821 20. Pandit, S.K. et al. E2F8 is essential for polyploidization in mammalian cells. *Nature Cell*
822 *Biology*. **14** (11), 1181–1191 (2012).

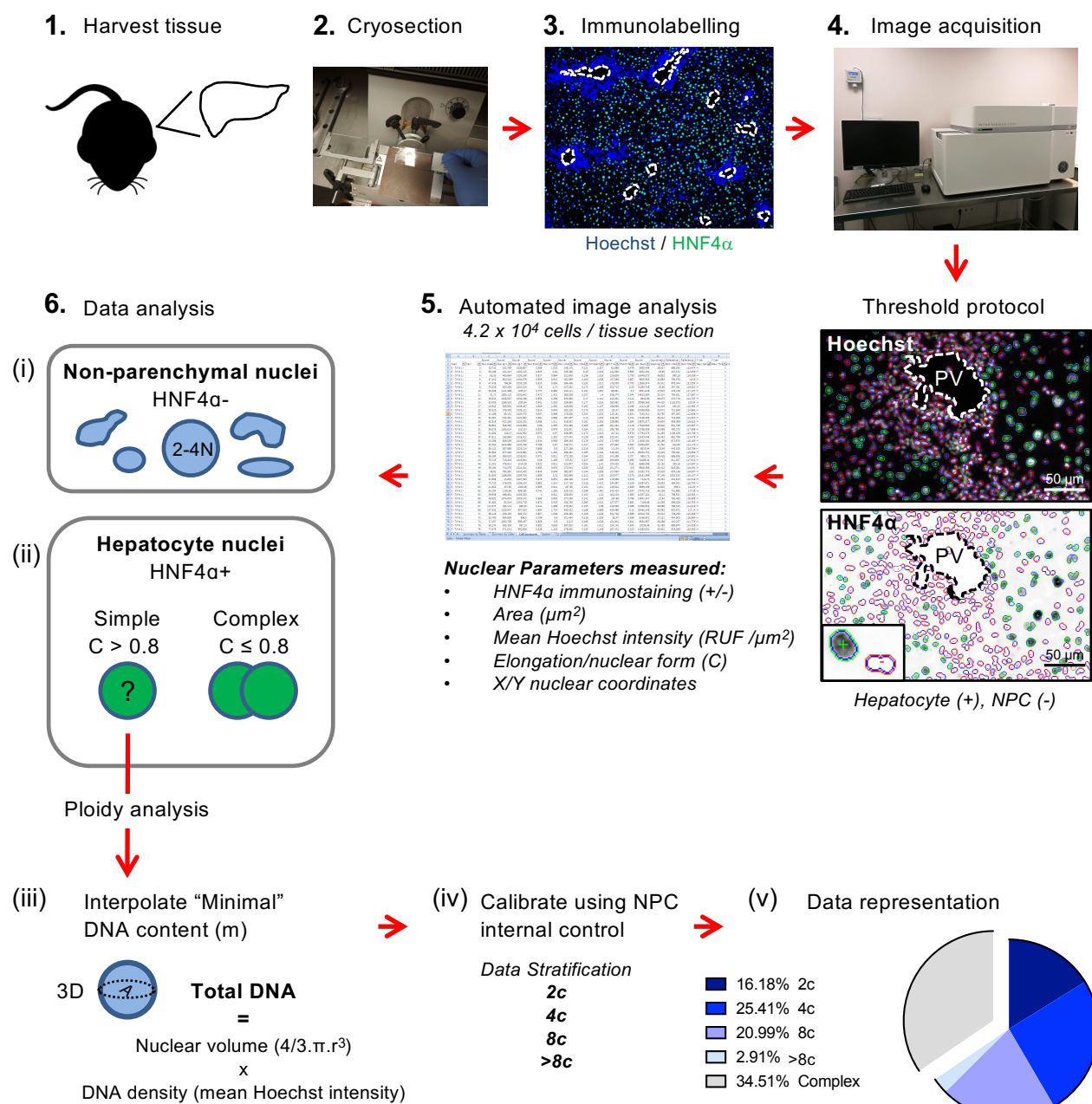
823 21. Vinogradov, A.E., Anatskaya, O. V., Kudryavtsev, B.N. Relationship of hepatocyte ploidy levels
824 with body size and growth rate in mammals. *Genome*. **44** (3), 350–360 (2001).

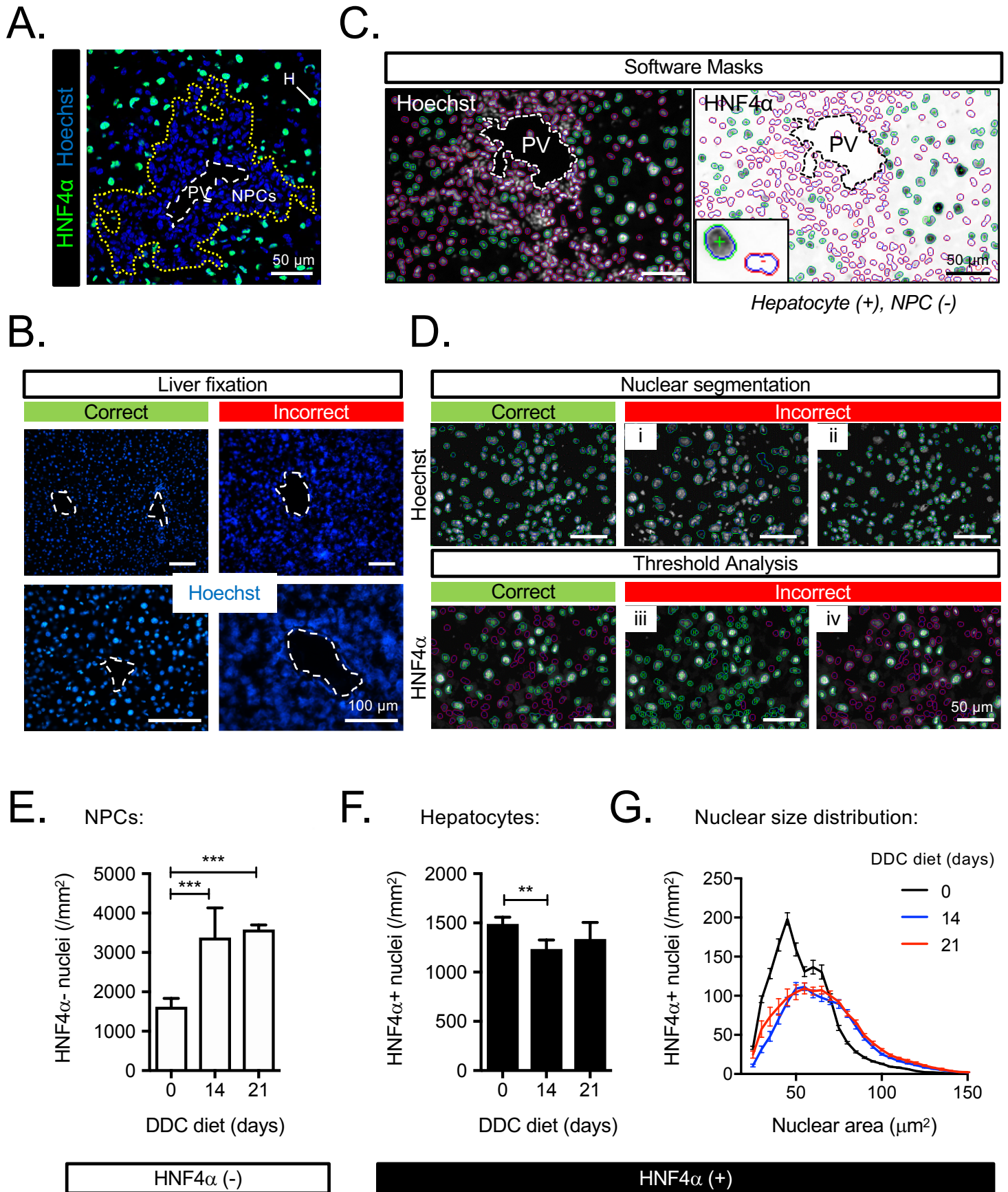
825 22. Tanami, S. et al. Dynamic zonation of liver polyploidy. *Cell and Tissue Research*. **368** (2), 405–
826 410 (2017).

827 23. Kudryavtsev, B.N., Kudryavtseva, M. V., Sakuta, G.A., Stein, G.I. Human hepatocyte
828 polyploidization kinetics in the course of life cycle. *Virchows Archiv B Cell Pathology Including*
829 *Molecular Pathology*. **64** (1), 387–393 (1993).

830 24. Gentric, G., Celton-Morizur, S., Desdouets, C. Polyploidy and liver proliferation. *Clinics and*
831 *Research in Hepatology and Gastroenterology*. **36** (1), 29–34 (2012).

832 25. Uhlén, M. et al. Tissue-based map of the human proteome. *Science*. **347** (6220), 1260419–
833 1260419 (2015).

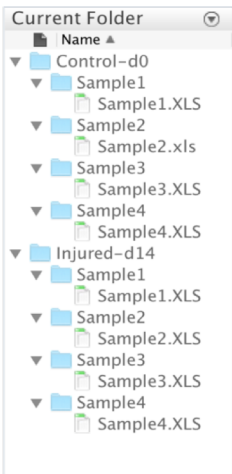




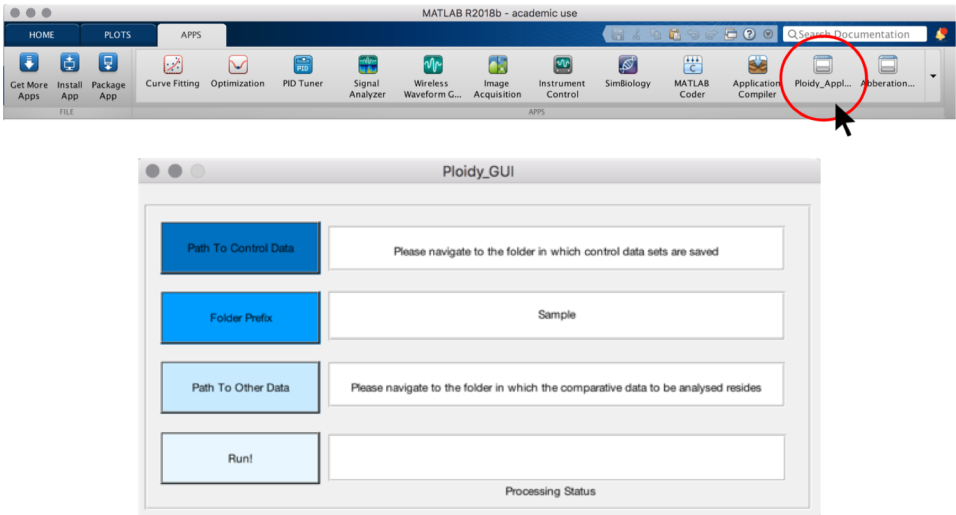
A

	A	B	C	D	E	F	G	H	I	J	K	L	M	N	O	P	Q	R
			Nuclei	Nuclei	Nuclei	Nuclei	Nuclei	Nuclei	Nuclei	Nuclei	Nuclei	Nuclei	Nuclei	Coordination	Reference 1	Reference 2	Filter	Filter
1	Well	Cell	Nuc Area	Nuc cg X	Nuc cg Y	Nuc Elongation	Nuc 1/(Form Factor)	Nuc Intensity	Nuc Intensity CV	Compactness	Light Flux	Chord Ratio	IxA (Nuc)	Spacing (SOI)	Nuc Intensity	Nuc Intensity	New Decision Tree	New Threshold
2																		
3	0	1	32.865	228.063	1034.316	0.994	1.025	269.861	0.154	1.095	121.229	0.462	8869.095	16.409	169.38	113.709	—	0
4	0	2	23.297	267.268	1037.232	0.408	1.201	294.804	0.157	1.481	90.729	0.339	6868.047	16.941	908.964	115.518	H	1
5	0	3	37.858	419.758	1034.648	0.74	0.985	242.022	0.177	1.097	145.459	0.5	9162.388	44.109	181.077	115.044	—	0
6
7																		
8																		
	Cell measures		+															

B

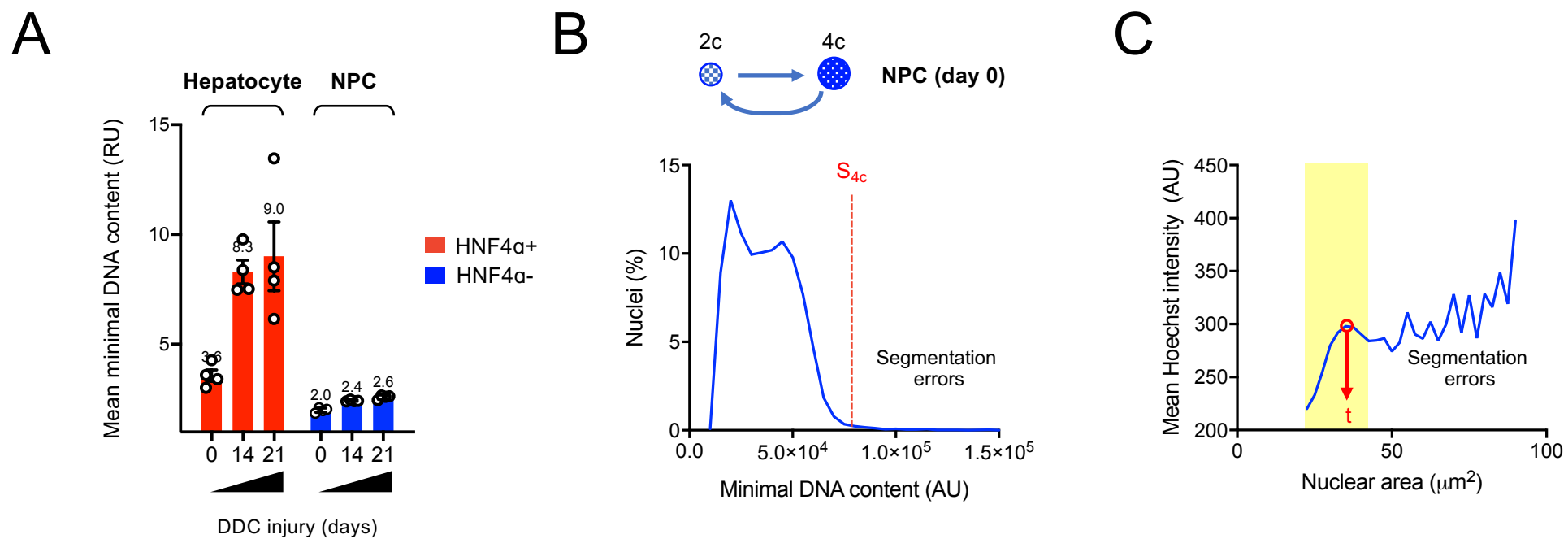


C

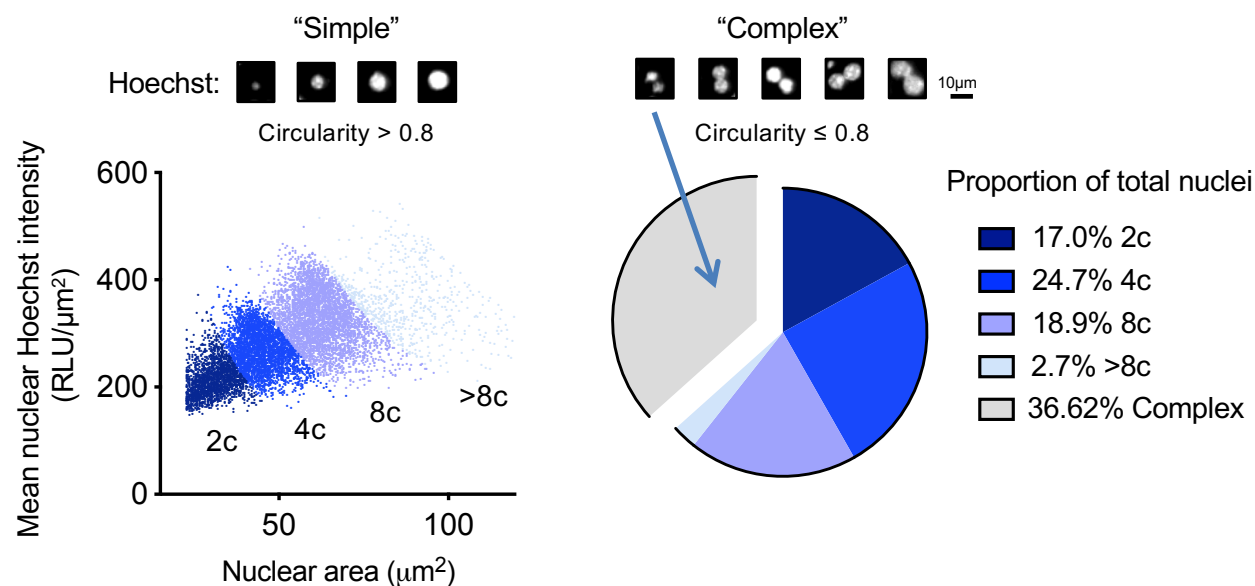


D

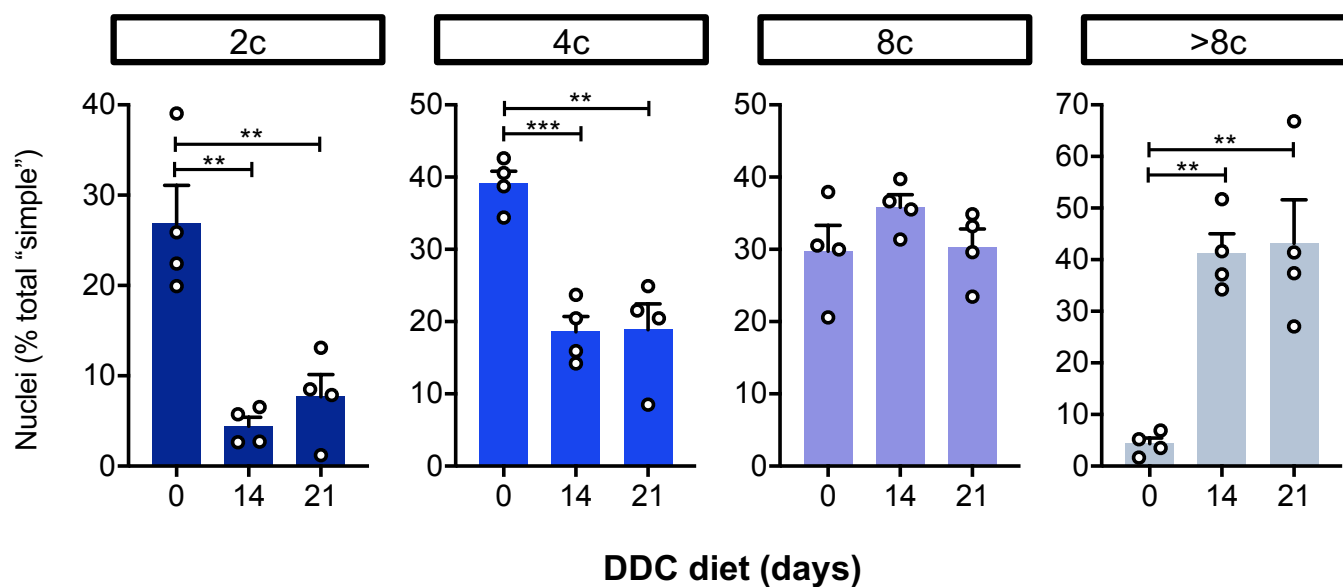




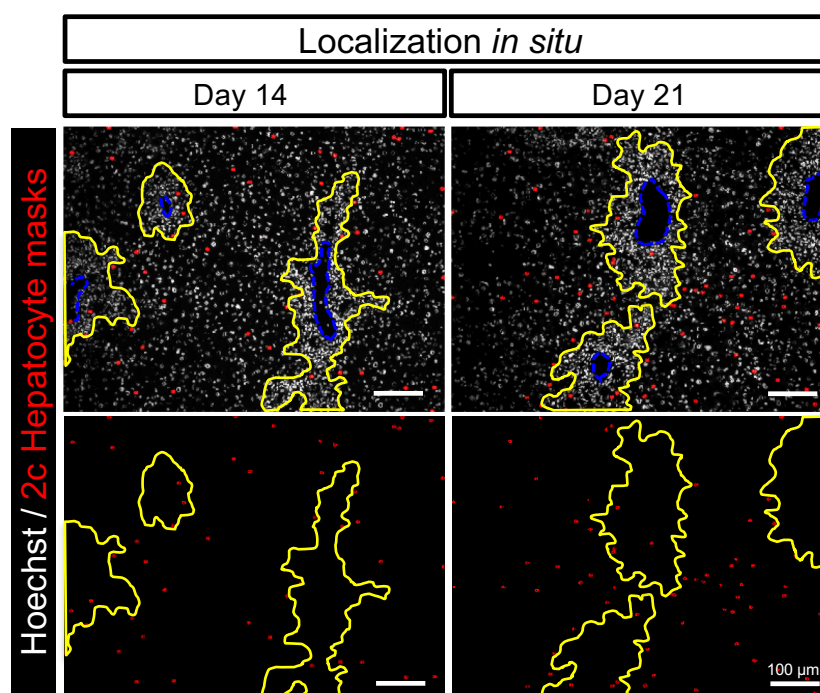
A.

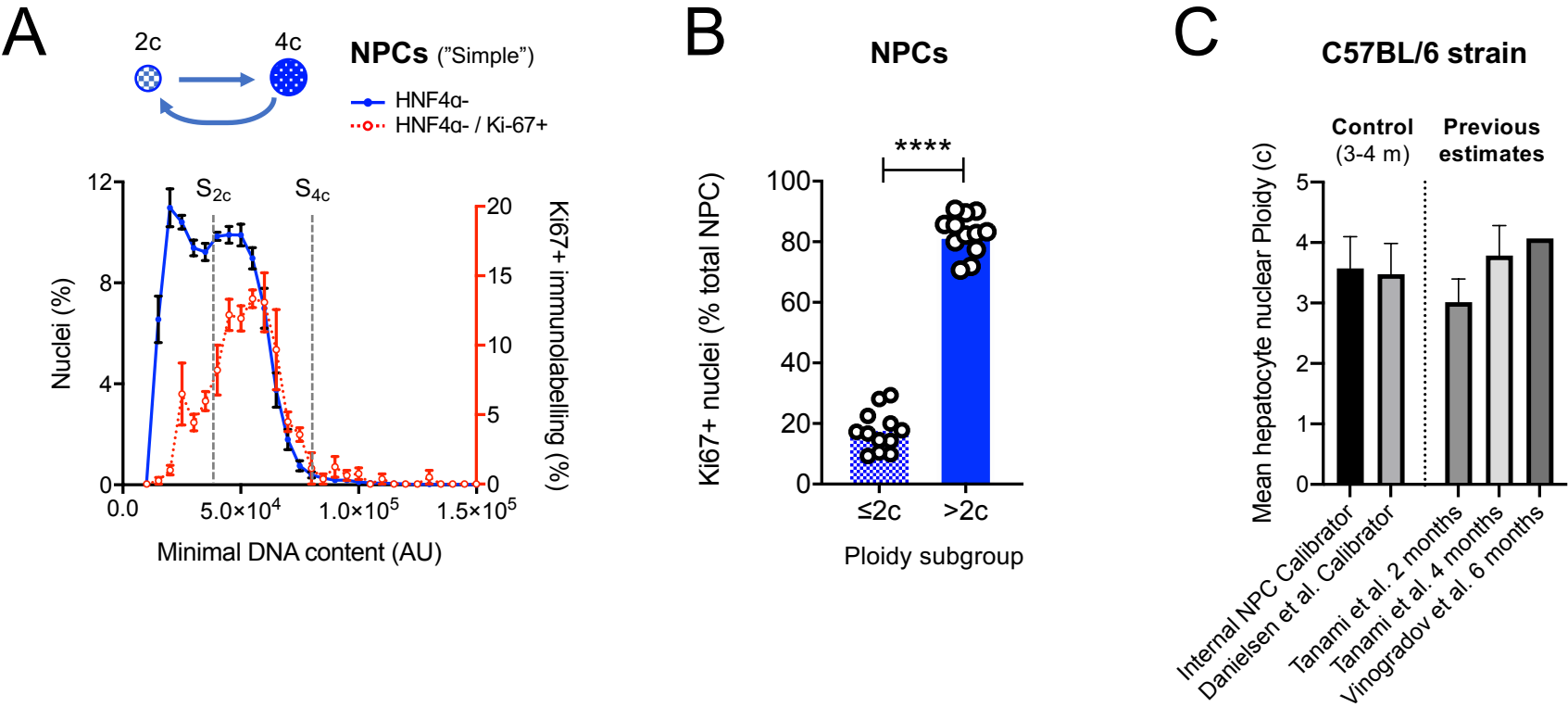


B.

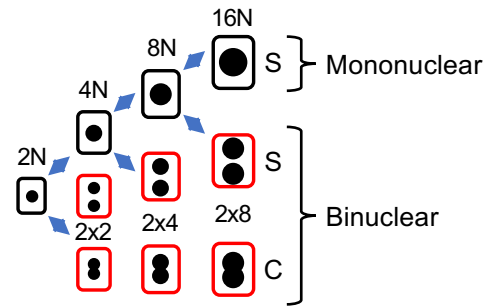


C.





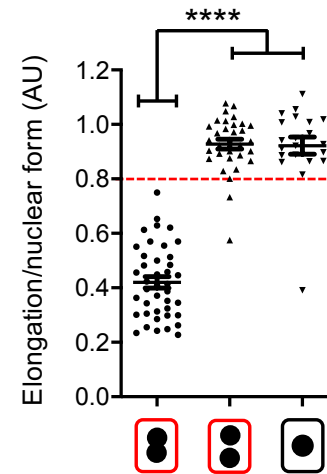
A

**Nuclear Morphometry:**

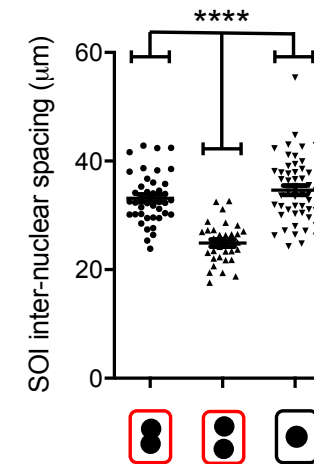
S = "simple" (circularity >0.8)

C = "complex" (circularity ≤0.8)

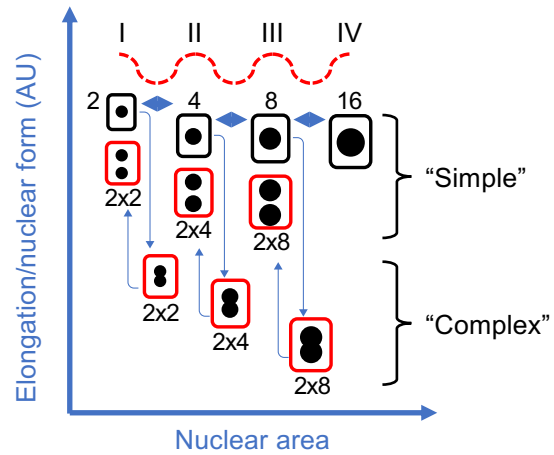
B



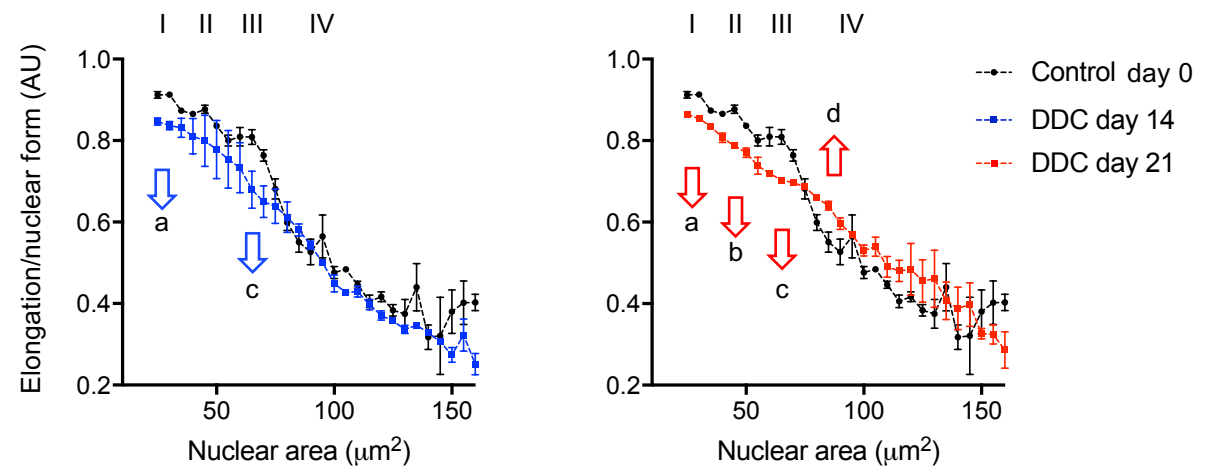
C



D



E



Name of Material/Equipment	Company	Catalog Number	Comments/Description
3,5-diethoxycarboxynl-1,4-dihydrocollidine diet (DDC)	TestDiet	1810704	Modified LabDiet mouse diet 5015 with 0.1% DDC
Alexa Fluor 488 donkey anti-goat IgG (H+L)	Invitrogen	A11055	Dilution 1:500
Bovine Serum Albumin	Sigma-Aldrich	A7906	Tissue sectioning
Cryostat Leica CM1850 UV	Leica biosystems	CM1850 UV	
Fluorescent Mounting medium	Dako	S3023	
GraphPad Prism	GraphPad Software	Prism 8	Statistical software for graphing data
Hoechst 33342	Sigma-Aldrich	B2261	Final concentration 5 µg/mL
IN Cell Analyzer 1000	GE Healthcare Bio-Sciences Corp		High-Content Cellular Imaging and Analysis System
MATLAB	MathWorks	R2019a	Data analytics software for automated analysis of nuclear ploidy
Microscope coverslides	VWR International	630-2864	Size of 24 x 60 mm
Microsoft Office Excel	Microsoft		Spreadsheets software
OCT Tissue Tek	Pascual y Furió	4583	
Paraformaldehyde	Panreac AppliChem	141451.121	
Pen for immunostaining	Sigma-Aldrich	Z377821-1EA	5mm tip width
Polysine Microscope Slides	VWR International	631-0107	
Rabbit polyclonal Anti-HNF4α	Thermo Fisher Scientific	PA5-79380	Dilution 1:250 (alternative)
Rabbit polyclonal Anti-HNF4α	Santa Cruz Biotechnology	sc-6556	Dilution 1:200 (antibody used in the study)
Tween 20	Sigma-Aldrich	P5927	

This piece of the submission is being sent via mail.

RE: Rebuttal document for revision due Dec 17, 2019

Ref: JoVE60095

Title: “A high-throughput in situ method for estimation of hepatocyte nuclear ploidy in mice”

Dear Editor,

The following document contains a comprehensive response to both the editorial and reviewer comments. The authors comments are highlighted (*in red*).

Sincerely,

Dr. Luke A. Noon

Editorial comments:

Please note that the editor has accepted all changes in the submitted revision to obtain a clean version of the manuscript. All editorial and reviewer comments are made on this clean version (see the attachment) and please use this updated version for future revisions.

Changes to be made by the author(s):

1. 1.1: Please specify the age, gender and type of animals used here.

- *The following text has been added to step 1.1: “(all analyses have been performed using adult female C57BL/6 mice aged 12-16 weeks)”*

2. 5.3: Please specify the parameters used here.

- *Step 5.3 and the note below have been edited to provide a clear description of these parameters*
- *The values for minimal nuclear area and nuclear detection sensitivity used in the study are now provided in the NOTE below step 5.3 and we also offer a more detailed description of the nuclear size range of hepatocytes and non-hepatocytes in the mouse liver*
- *Figure 2D and the corresponding figure legend have been modified to help describe in more practical terms how these parameters should be altered to achieve optimal nuclear segregation and thresholding for HNF4 α .*

3. 5.4: Please specify the threshold intensity used here.

- *The value of threshold intensity is relative and will depend on staining efficiency and acquisition settings such as laser intensity. It should therefore be standardized by the user.*
- *We have added the text above to “CRITICAL STEP” section beneath step 5.4. “*

4. Section 6.3: In the accompany video, will you demonstrate the analysis using your software? If so, software steps must be more explicitly explained ('click', 'select', etc.). Please add more specific details (e.g., button clicks or menu selections for software actions, numerical values for settings, etc.). For instance, combine the details regarding how to run the application in the supplemental file (section 2.3) with explanations of each step in section 6.3.

- *Thank you for this comment. We agree with the editor that the new software is overlooked in the current protocol. In the video, we intend to demonstrate the analysis using the software. We have now edited the protocol as requested to add explicit steps showing how to install, input data and run the application (new steps 6.3.1 to 6.3.3 adapted from the supplementary document as suggested). A new Figure 3 has also been added, which contains screenshots illustrating data formatting, software usage and data output, and we have changed the highlighted yellow text accordingly. We feel that the changes made greatly simplify the methodology for the reader and helps bring the custom written program to centre stage.*

5. Are any figures reprinted from a previous publication? If so, please obtain explicit copyright permission to reuse any figures from a previous publication. Explicit permission can be expressed in the form of a letter from the editor or a link to the editorial policy that allows re-prints. Please upload this information as a .doc or .docx file to your Editorial Manager account. The Figure must be cited appropriately in the Figure Legend, i.e. “This figure has been modified from [citation].”

- *The Figure 2 legend has now been changed as recommended to state that “This figure has been modified from”. The data used in this figure comes from our PLOS Biology publication which has a Creative Commons License which enables free distribution. Please advise as to whether any further permission is required*

6. Figures: Please include a space between the number and the units of the scale bar. Please delete the space before the percent sign.

- *Spaces between the units and scale bar have now been checked and added in all figures*
- *Spaces before % in Figure 4 have been deleted*

7. References: Please include volume, issue as well as page number for each reference.

- *References have been edited to include volume, issue and page number*

Reviewers' comments:

Reviewer #2:

i am happy with the revise manuscript.

Reviewer #5:

Manuscript Summary:

The authors present here a new method to analyze and quantify nuclear ploidy in hepatocytes in fixed/cryopreserved tissue samples. This method is described as alternative to standard flow cytometry techniques requiring cell disaggregation and the consequent loss of spatial information.

The protocol is based on the identification of hepatocytes by immunofluorescence staining with an anti-HNF4 antibody, acquisition of fluorescence images by a high-content imaging platform and analysis of hepatocyte nuclear size distribution and ploidy to distinguish different subsets of hepatocytes. As internal control, the analysis of non-parenchymal cells has been proposed and utilized.

I believe that the proposed method is interesting and useful for the analysis of ploidy in fixed tissues from normal or injured/transformed livers. This protocol could allow the analysis of ploidy changes of hepatocyte population in during liver injury, regeneration and neoplastic transformation.

The morphometric parameters utilized can efficiently characterize different hepatocytes subpopulations "in vivo". Furthermore, data presented by the authors, where the protocol has been used to analyze the impact of cholestatic injury on adult mouse livers, is convincing and supports the efficacy of the protocol.

- *RESPONSE: We thank Reviewer#5 for their positive feedback and constructive comments. In the revised manuscript we have sought to address all of the reviewers concerns. Please find below a detailed breakdown of our actions:*

Major Concerns:

- while the protocol of tissue preparation and labelling does not require complex procedures, the analysis of data from morphometric measures appears tricky and dependent on the operator's ability, especially in the set-up of the parameters (more than a flow cytometry analysis), and therefore not easy to be managed. The authors should add a comment about the eventual request of a specific expertise, need of skilled operators, variance due to the operator's discretion in the choice of nuclear masks.

- *A sentence has been added to the introduction of step 5, which highlights the need for "some basic operator training/expertise" for optimal segmentation and thresholding.*
- *Extra detail has been added to the notes beneath steps 5.3 and 5.4 to further stress the role of the operator and help the user standardize the set up procedure. This includes providing reference values for expected nuclear size and minimal size cut-off.*

- In the new figure 4B the statistical analysis has changed compared to the original figure 3B. Has new data been included? The authors should explain this discrepancy.

- *We apologize for the confusion. No new data was included in figure 4B. In the original version of the manuscript, the calibration method for calculating nuclear ploidy used an external descriptor of 2n hepatocyte nuclear size that Reviewer#3 asked us to remove. In the revised manuscript, the calibration method was improved so that it did not require this external information. Given the change in calibration method, the ploidy estimates using the same data differ slightly, explaining the discrepancy in statistical analyses identified by Reviewer#5.*

- The sections from 6.3.3.1 to 6.3.3.5 appear unclear and should be better explained

- *These 5 steps (now 6.3.4.3.1 to 6.3.4.3.3) have now been edited and the language has been altered to make the calibration methodology clearer.*

- the difference between "nuclear elongation factor" and "nuclear form factor" is not clearly defined. Furthermore, the calculation of "circularity index" should be better explained with examples since it is a key parameter to distinguish hepatocytes with different ploidy.

We thank the reviewer for this comment and agree that it is important to improve the clarity of the description of nuclear circularity in the manuscript:

- *New Definitions of "nuclear elongation factor" and "nuclear form factor" have now been added in step 5.5*

- A note has been added at the foot of step 6.3.4.1.1 (previously 6.3.1.1) to provide a clear definition of the “circularity index” used to separate “simple” and “complex” nuclei. It reads:
 - NOTE: “Nuclear elongation” and “Nuc 1/(form factor)” are two discrete measures of an object’s “circularity” that assess complementary, non-overlapping morphometric criteria. The former measures the long- and short-axes of an object, whilst the latter compares the length of perimeter of an object to that of its area. To strengthen the definition of nuclear circularity used in this protocol, these two measurements have been combined into a single “circularity index”. A previous approach to estimate nuclear ploidy using the described methodology used only nuclear elongation¹⁷. Whilst acceptable results were obtained using this approach, the authors have observed that a composite “circularity index” improves discrimination of manually selected nuclei from mononuclear and binuclear hepatocytes (data not shown)
- The “data not shown” referred to in the NOTE above are provided below (in “Figure X”) for the appraisal of the Reviewer. Use of the combined “circularity index” (B) improves the categorization of manually selected binuclear cells with “touching nuclei” as compared to nuclear elongation alone (A) – increasing correct classification from 73.2% to 100%.

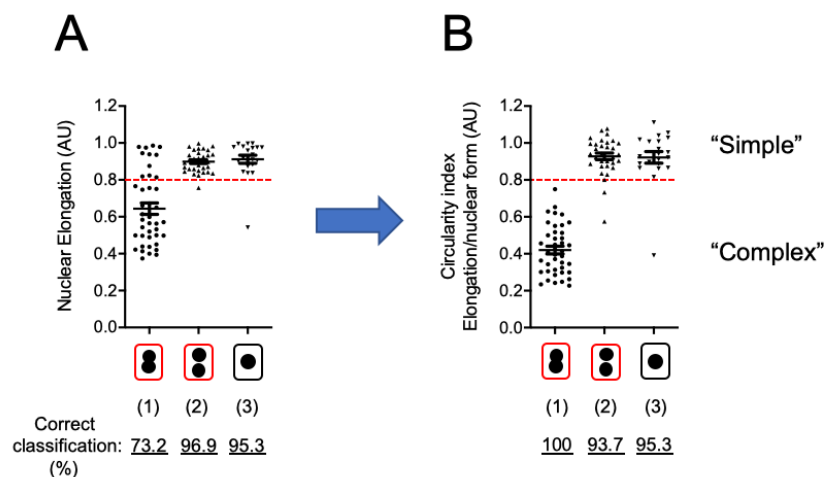


Figure X – Manually selected hepatocytes with either “complex” (1) or “simple” nuclei (2&3) were classified by nuclear morphometry according to: (A) Nuclear Elongation alone, or (B) the combined “circularity index” described in our protocol. Using the same threshold (indicated by red dotted line), the data show an improved segregation of complex binuclear hepatocytes (1) from simple mononuclear cells (3) in (B). Dots represent individual HNF4α-positive nuclei.

Minor Concerns:

- a minimal editing of text is required. In particular, two sentences in Introduction (lines 60-64 and lines 74-78) and in Protocol (lines 326-328 and 338-343) need to be revised.

- Sentence 60-64 has been shortened and edited
- Sentence 74-78 has been broken up and edited
- Reference to (lines 326-328 and 338-343) was difficult to find. However, calibration steps previously named 6.3.3.2 to 6.3.3.6 have been revised in response to the major concern (above) .

- change “;” in line **31** and line **223** with “.”

(done)

- change “;” in line **74** with “ that is”

This sentence has been edited and improved to remove “;”

- change “means” in line **84** with “method”

(Done)

- lines **251-253**: "Nuc1" and "center of gravity" terms need to be briefly explained

(Done)

Reviewer #6:

Manuscript Summary:

The manuscript by Manzano-Nunez and colleagues provides an excellent method to quantify in situ hepatocyte nuclear ploidy within liver parenchyma. Although known for long time polyploidy indeed is a fascinating characteristic of the liver parenchyma that still covers many important topics to be revealed and to be extremely important. Polyploid hepatocytes are characterized by the number of nuclei per cell (cellular ploidy), as well as the ploidy of each nucleus (nuclear ploidy). The manuscript accurately described in detailed the method to analyze nuclear ploidy. This method has been used to measure the impact of cholestatic injury on the adult mouse liver. The text is well written, clear and free of bias. The figures are clear.

- *RESPONSE: We thank Reviewer#6 for their generous appraisal of the manuscript and for recognizing the potential importance of our protocol to research in this field . Please find below a detailed response to their useful suggestions and comments:*

Minor Concerns:

I only have a few minor suggestions:

1) Maybe at the end of the manuscript, it will be interested to discuss what is advantage of this new method compared to others methods that have been already published to quantify hepatocyte nuclear ploidy in mice.

Gentric G, Maillet V, Paradis V, Couton D, L'Hermitte A, Panasyuk G, et al. Oxidative stress promotes pathologic polyploidization in nonalcoholic fatty liver disease. J Clin Invest 2015;125:981-92.

Miyaoka Y, Ebato K, Kato H, Arakawa S, Shimizu S, Miyajima A. Hypertrophy and unconventional cell division of hepatocytes underlie liver regeneration. Curr Biol 2012;22:1166-75.

Tanami S, Ben-Moshe S, Elkayam A, Mayo A, Bahar Halpern K, Itzkovitz S. Dynamic zonation of liver polyploidy. Cell Tissue Res 2017;368:405-10.

Morales-Navarrete H, Segovia-Miranda F, Klukowski P, Meyer K, Nonaka H, Marsico G, et al. A versatile pipeline for the multi-scale digital reconstruction and quantitative analysis of 3D tissue architecture. Elife 2015;4.

- *We thank Reviewer#6 for this very useful suggestion. In response, we have added two sentences to the discussion (underlined) to elaborate the advantages of our method:*

"An important innovation is the use of NPCs as an internal ploidy calibrator that enables relative assessment of hepatocyte nuclear DNA content both within and between samples. Incorporation of an HNF4 α labelling step is therefore key to providing this protocol with a unique technical advantage compared to previously published 2D methods^{3,12,22}. In contrast, the relative simplicity of the methodology in comparison with 3D reconstruction workflows¹⁸ makes it technically less laborious and potentially more flexible."

2) As described in the paper, there is an age-dependent difference in hepatocytes nuclear ploidy. For the experiments, the authors have used adult female C57BL/6 mice aged 12-16 weeks. Do the authors have analyzed if they can quantify by their method nuclear ploidy modification during normal ageing? Is there a difference of nuclear ploidy between adult male and female C57BL/6 mice (same age)?

- *Unfortunately, we have not investigated age or sex dependent changes in nuclear ploidy using our methodology and agree with the reviewer that this would be interesting. Both age and sex dependent differences in hepatocyte nuclear ploidy in C57BL/6 mice have been described previously by Ohtsubo et al (1986) using FACS. This study showed that nuclear ploidy increased in both males and females with age, but that young (<5months) male mice had nearly twice the number of 4C nuclei compared to females of the same age*

Ohtsubo, K. & Nomaguchi, T. A. A flow cytofluorometric study on age-dependent ploidy class changes in mouse hepatocyte nuclei. Mechanisms of Ageing and Development (1986).doi:10.1016/0047-6374(86)90013-8

3) With this methods, do the authors are able to define nuclear ploidy within binuclear fraction (2x2N, 2x4N, 2x8N) in normal liver parenchyma.

- *As we have outlined in the “Interpretation of nuclear morphometry” section of the manuscript, our methodology cannot clearly discriminate between the nuclei of mononuclear hepatocytes and those of binuclear cells in which the nuclei are clearly separated within a common cytoplasm. This limitation and how it could potentially be overcome are discussed in “Future refinements and challenges”.*
- *Within this discussion we state that: “further segregation of “complex” binuclear cells could be achieved by radial measurements of the nuclei that their 2D masks contain”. In other words, we think that it is conceivable that morphometric interrogation of “complex” nuclei could reveal quantitative data relevant to the numbers of 2x2N, 2x4N and 2x8N binuclear cells as suggested by the reviewer.*

Nuclear ploidy analysis software

From: JoVE60095 “A high-throughput in situ method for estimation of hepatocyte nuclear ploidy in mice”

The post-processing described in step 6.3.4 of the protocol (JoVE60095) can be performed using a custom written MATLAB application, freely available for download at : <https://github.com/lukeynoon>. Source code is also provided for users who wish to adapt the methodology. The following section describes the methodology and use of the application for the estimation of nuclear ploidy. Please report any user issues on the GitHub site. Alternatively, please contact rp649@cam.ac.uk or lnoon@cipf.es under the subject line of Ploidy Application.

1.1 Description of the methodology

The algorithm uses nuclear morphometry data to firstly separate hepatocyte nuclei into two groups; (1) those with “simple” circular nuclei and (2) “complex” non-circular nuclei representative of binuclear cells with >2c ploidy. The minimal nuclear DNA content (a function of nuclear area and DNA density) is next calculated. A subsequent step then calibrates HNF4α+ hepatocyte nuclear ploidy using HNF4α- nuclei as a known 2-4N internal control. A summary of the steps taken by the software are outlined below:

1.1.1 Separate the control data into “simple” or “complex”

1.1.1.1. Data is automatically separated into either HNF4α+ or HNF4α- nuclei.

1.1.1.2. A circularity index (defined as the Elongation divided by the Form Factor) is calculated for all nuclei.

1.1.1.3. Nuclei for which the circularity index ≤ 0.8 or >0.8 are classified as “complex” and “simple” respectively. Note that a value of 1.0 indicates a perfect circle.

1.1.2. Estimate the minimal nuclear DNA content of simple hepatocytes and non-parenchymal cells within the control data

1.1.2.1 The method estimates the nuclear radius (r) of both simple hepatocyte and non-parenchymal nuclei by:

$$r = \sqrt{\frac{\text{nuclear area}}{\pi}}$$

1.1.2.2. The nuclear volume (v) is then calculated per:

$$v = \frac{4}{3} \times \pi \times r^3$$

1.1.2.3. From which a relative value of minimal DNA content is estimated as:

$$\text{minimal DNA content} = \text{Mean Hoechst intensity} \times v$$

1.1.3 Stratify minimal DNA content of “simple” nuclei according to ploidy (2c, 4c, 8c or 16c) by calibrating the dataset using non-parenchymal nuclei as an internal 2-4n control.

1.1.3.1. A histogram of the minimal DNA content of the HNF4α- nuclei is computed. Bin width is set to the square root of the number of values binned.

1.1.3.2. An average of the three most frequent bins in the histogram is used as an estimation of the modal value of the Nuclear DNA content.

1.1.3.3. The minimal DNA contents are then filtered to those that lie within 1 standard deviation of this average value.

1.1.3.4. Within this filtered range, the nuclear areas and corresponding Hoechst intensities are examined. The minimum size for which the Hoechst intensity is maximum is extracted (defined here as the minimum of the second derivative of the area vs. Hoechst intensity curve). This represents the 2n-4n transitional state.

1.1.3.5. To estimate the 4n shoulder, 1 standard deviation of the Nuclear DNA content is appended to the transitional point.

1.1.3.6 Steps **1.1.3.1 – 1.1.3.5.** are repeated for all Control samples.

1.1.3.7. An average 4c stratification threshold is calculated, from which the 2c (S_{2c}) and 8c (S_{8c}) boundaries for minimal DNA content (m) are further estimated.

1.1.3.8. The corresponding ploidy value of each nucleus is calculated per:

$$Ploidy (p) = \frac{Minimal\ DNA\ content\ (m)}{S_{2c}} \times 2$$

For which S_{2c} represents the 2c DNA content standard, i.e. the 2n stratification threshold calculated in section **1.1.3.7.**

1.1.3.9. Ploidy values (p) of non-parenchymal cells are automatically saved and simple hepatocyte nuclei are stratified into 2c/ 4c / 8c/ 8c+ ploidy brackets according to the following criteria:

"2c"	Hepatocytes =	p	≤ 2
"4c"	Hepatocytes =	2 < p	≤ 4
"8c"	Hepatocytes =	4 < p	≤ 8
"8c+"	Hepatocytes =	8 < p	

1.1.4 Ploidy estimation and stratification for comparative (e.g. Injured) samples.

1.1.4.1. Steps **1.1.1 – 1.1.2** are repeated for the comparative data sets.

1.1.4.2. The comparative data sets are stratified according to the control thresholds calculated in section **1.1.3.7.**

1.1.4.3. The corresponding ploidy value of each cell is calculated and stratified per sections **1.1.3.8 – 1.1.3.9.**

2.1 Installing the application

2.1.1 Download the packaged application from : <https://github.com/lukeynoon>

2.1.3 Launch MATLAB.

2.1.3 Navigate to the APP tab of the MATLAB toolstrip, click "Install App" and open the downloaded application termed "*Ploidy_Application.mlappinstall*". A message will appear to confirm the successful installation.

2.1.4 The application is now ready for use and will remain in the APP tab of the MATLAB toolstrip.

2.2 Critical stages before running the application: Data must be stored according to the following instructions.

2.2.1 The exported excel spreadsheet files (.XLS 97-2004 workbook) from the high-content image analysis software must contain a sheet termed “Cell measures” which contains the data required for the ploidy analysis. It is important that the following column header names remain unchanged (see example datasets), as the analysis method finds the correct column data by searching for these names. If for example, your software does not produce a “Light flux” column shown here in column K, please manually insert a column termed “Light flux” in the same location, i.e. column K and fill it with zeros.

	A	B	C	D	E	F	G	H	I	J	K	L	M	N	O	P	Q	R
1			Nuclei	Nuclei	Nuclei	Nuclei	Nuclei	Nuclei	Nuclei	Nuclei	Nuclei	Nuclei	Nuclei	Coordination	Reference 1	Reference 2	Filter	Filter
2	Well	Cell	Nuc Area	Nuc cg X	Nuc cg Y	Nuc Elong	Nuc 1/For	Nuc Intens	Nuc Intens	Compactn	Light Flux	Chord Rat	IxA(Nuc)	Spacing (S	Nuc Intens	Nuc Intens	New Decis	New Thres

2.2.2 For each experimental condition, a control data set must be provided since this will be used to calculate the internal control (see **1.1.3**). In this study, we used normal livers from untreated adult littermates (“Control-d0”).

2.2.3 For biological replicates (per condition), each excel spreadsheet should be stored in its own folder. The folder prefixes should be named incrementally, for example as “Sample1, Sample2, Sample3.... SampleN”, as per the filenames. For example, your data should be stored in this way:

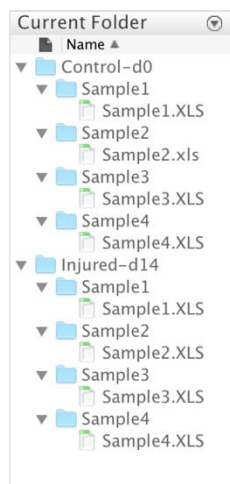


Figure: Example of data storage requirements.

2.3 Running the application.

2.3.1 Click on the Ploidy_Application via the MY APPS tab of the MATLAB toolstrip:



Figure: Launching the Ploidy_Application.

2.3.2 The Ploidy_Application GUI will appear:

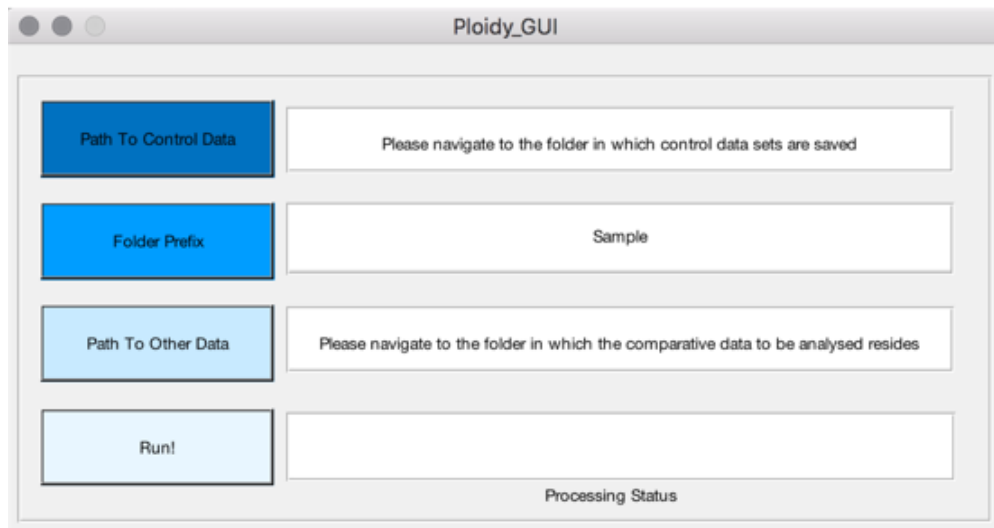


Figure: Ploidy_Application GUI.

2.3.4 Click the “Path to control data” button to navigate to the folder in which the control data replicates reside. This data path will then appear in the interface. For example, in the case of **section 2.2.3** this data path would be: */Users/Desktop/Control-d0*

2.3.5 Next, type the name of the folder/file pre-fix names chosen. For example, in the case of **section 2.2.3** this would be: *Sample*. Note that this prefix can be changed to any text, provided that the folders and filenames remain incrementally named.

2.3.6 Click the “Path to other data” button to navigate to the folder in which the comparative data replicates reside. This data path will then appear in the interface. For example, in the case of **section 2.2.3** this data path would be: */Users/Desktop/Injured-d14*

2.3.7 Click the “Run!” button. When the analysis is complete, the status bar will read “Analysis Complete!..”

2.4 Application Outputs

2.4.1 The application will report, for each sample, stratification into $\leq 2n$, $2n-4n$, $4n-8n$ and

8n+ in terms of absolute counts and as a percentage of total. These files will be automatically saved in each sample folder as:

"Count_2n.txt"
 "Count_2n_to_4n.txt"
 "Count_4n_to_8n.txt"
 "Count_8n_and_higher.txt"
 "Percentage_2n.txt"
 "Percentage_2nto4n.txt"
 "Percentage_4nto8n.txt"
 "Percentage_8n_and_higher.txt"

2.4.2 The application will automatically save, for each sample, the ploidy estimation for hepatocytes and non-hepatocytes as:

"Ploidy_All_Hepatocytes.txt"
 "Ploidy_NonHepatocytes.txt"

2.4.3 For the control data set, the method also saves the thresholds used for the stratification (section 1.1.3) in a file termed "Normalised_Thresholds_Control".

2.4.4 Finally, the application will produce a folder for the control and the other condition data termed "Summary". This folder contains two subfolders: "Ploidy" and "Stratification" which contain the averages of all samples provided:

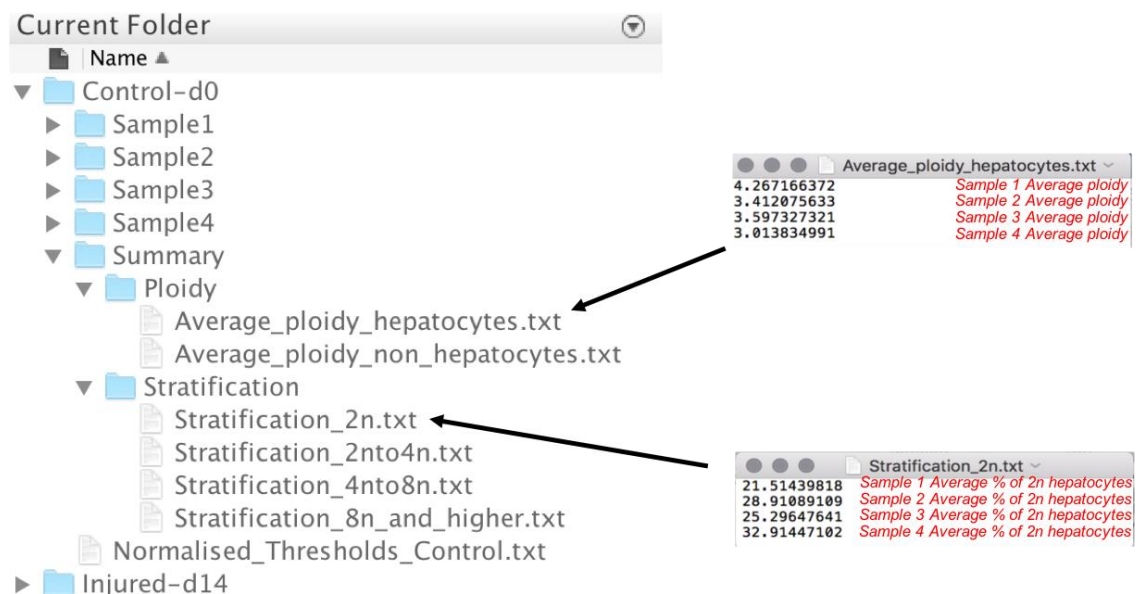
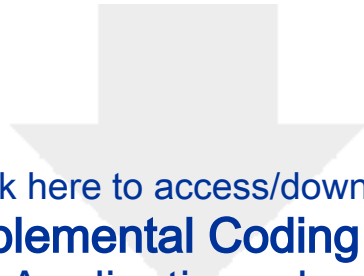


Figure: Example of the summary output files of the Ploidy Application.



[Click here to access/download](#)

Supplemental Coding Files
Ploidy Application.mlappinstall

